EUROPEAN ORGANIZATION FOR NUCLEAR RESEARCH (CERN)

FERMILAB-PUB-15-275-CMS

CERN-PH-EP/2015-133
2015/06/30

CMS-HIG-14-017

Search for neutral MSSM Higgs bosons decaying into a pair of bottom quarks

The CMS Collaboration*

arXiv:1506.08329v1 [hep-ex] 27 Jun 2015

Abstract

A search for neutral Higgs bosons decaying into a $b\bar{b}$ quark pair and produced in association with at least one additional b quark is presented. This signature is sensitive to the Higgs sector of the minimal supersymmetric standard model (MSSM) with large values of the parameter $\tan\beta$. The analysis is based on data from proton-proton collisions at a center-of-mass energy of 8 TeV collected with the CMS detector at the LHC, corresponding to an integrated luminosity of $19.7\,\mathrm{fb}^{-1}$. The results are combined with a previous analysis based on 7 TeV data. No signal is observed. Stringent upper limits on the cross section times branching fraction are derived for Higgs bosons with masses up to 900 GeV, and the results are interpreted within different MSSM benchmark scenarios, $m_{\mathrm{h}}^{\mathrm{max}}$, $m_{\mathrm{h}}^{\mathrm{mod+}}$, $m_{\mathrm{h}}^{\mathrm{mod-}}$, light-stau and light-stop. Observed 95% confidence level upper limits on $\tan\beta$, ranging from 14 to 50, are obtained in the $m_{\mathrm{h}}^{\mathrm{mod+}}$ benchmark scenario.

Submitted to the Journal of High Energy Physics

© 2015 CERN for the benefit of the CMS Collaboration. CC-BY-3.0 license

*See Appendix Appendix C for the list of collaboration members

Operated by Fermi Research Alliance, LLC under Contract No. De-AC02-07CH11359 with the United States Department of Energy.

1 Introduction

The discovery of a Higgs boson with a mass around 125 GeV [1–3] marked a milestone for elementary particle physics. While the measured properties of the observed boson are in agreement with the expectations of the standard model (SM) with the current experimental precision, this particle could well be the first visible member of an extended Higgs sector, which would be a direct indication of new physics. Extended Higgs sectors are possible in various theoretical models, such as Supersymmetry [4–7], which relates fermionic and bosonic degrees of freedom and in consequence requires the introduction of additional Higgs bosons as well as a superpartner to each SM particle. The superpartners provide potential dark-matter candidates [8], and their contribution to quantum-loop corrections can lead to a unification of the gauge couplings at higher energies [9]. Moreover, the problem of the quadratic divergence of the Higgs boson mass at high energies [10] is solved naturally through cancellation of loop terms by the superpartners.

The minimal supersymmetric extension of the SM (MSSM) [5] contains two scalar Higgs doublets, which result in two charged Higgs bosons, $H^{\pm}$, and three neutral ones, jointly denoted as ϕ. Among the latter are two CP-even (h, H) and one CP-odd state (A). The recently discovered boson with a mass near 125 GeV might then be interpreted as one of the neutral CP-even states. Two parameters, generally chosen as the mass of the pseudoscalar Higgs boson m_{A} and the ratio of the vacuum expectation values of the two Higgs doublets, $\tan\beta = v_2/v_1$, define the properties of the Higgs sector in the MSSM at tree level. For $\tan\beta$ values larger than one, the couplings of the Higgs field to down-type fermions are enhanced relative to those to the up-type fermions. Furthermore, the A boson is nearly degenerate in mass with either the h or H boson. These effects enhance the combined cross section for producing these Higgs bosons in association with b quarks by a factor of $\approx 2\tan^2\beta$. The decay $\phi \to \mathrm{b\bar{b}}$ is expected to have a high branching fraction ($\approx$90%), even at large values of the Higgs boson mass [11].

Measurements at the CERN LHC in the $\phi \to \tau\tau$ decay mode [12–15] have lead to the most stringent constraints on $\tan\beta$ so far, with exclusion limits in the range 4–60 in the mass interval of 90–1000 GeV. Preceding limits had been obtained by the LEP [16] and Tevatron experiments [17–19]. Besides extending the MSSM Higgs boson search to an independent channel, the $\phi \to \mathrm{b\bar{b}}$ decay mode is particularly sensitive to the higgsino mass parameter μ [20], and thus to the bottom quark Yukawa coupling. In the $\phi \to \tau\tau$ channel, the sensitivity to μ is much smaller due to a partial cancellation of the respective radiative corrections between the contributions to the production and decay processes [20]. Beyond the MSSM interpretation, lepton-specific two-Higgs-doublet models (2HDM) [21] may allow for enhanced couplings of down-type quarks relative to leptons. The $\mathrm{b\bar{b}}$ decay mode is also relevant in the more general context of exotic resonance searches, motivated for example by dark-matter models involving mediator particles with a large coupling to b quarks [22, 23].

Searches in the $\phi \to \mathrm{b\bar{b}}$ decay mode have initially been performed at LEP [16] and by the CDF and D0 experiments [24] at the Tevatron collider. The first and so far the only analysis at the LHC in this channel has been performed by the CMS experiment, using the 7 TeV data, and set significantly more stringent bounds in the mass range 90–350 GeV [25].

In this article, the CMS search is extended by adding the data set comprising 19.7 fb^{-1} of proton-proton collision data, collected at a center-of-mass energy of 8 TeV, and by the use of a refined methodology. The higher integrated luminosity as well as the greater center-of-mass energy allow extension of the search up to a mass of 900 GeV.

The search is performed for neutral MSSM Higgs bosons ϕ with masses $m_\phi \geq 100$ GeV that are

produced in association with at least one b quark and decay to $b\bar{b}$; an illustration of the signal process is given by the diagrams in Fig. 1. The signal is thus searched for in final states characterized by at least three b-tagged jets. No requirement of a fourth b-tagged jet is made, since its kinematic distributions extend significantly beyond the available acceptance in pseudorapidity, and the resulting signal efficiency would be very low. Events are selected by specialized triggers that identify b jets already at the online level. This is important to suppress the large rate of multijet production at the LHC. The analysis searches for a peak in the invariant mass distribution of the two b jets with the highest p_T values, which are assumed to originate from the Higgs boson decay. The dominant background is the production of heavy-flavor multijet events containing either three b jets, or two b jets plus a third jet originating from either a charm quark, a light-flavor quark or a gluon, which is misidentified as a b quark jet. For the final limits, the results of the 8 TeV analysis are combined with the previous 7 TeV analysis [25].

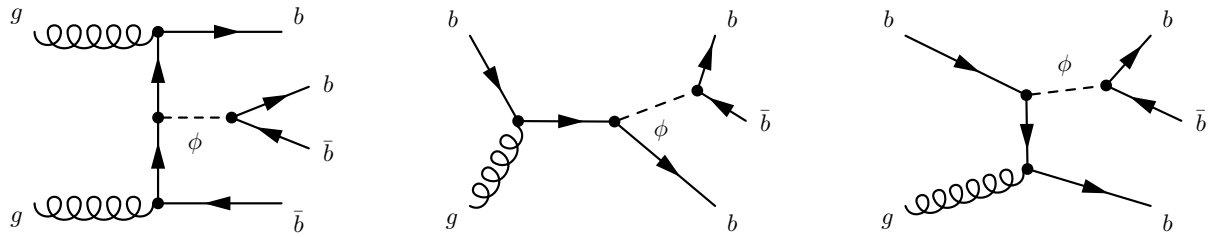

Figure 1: Example Feynman diagrams of the signal processes.

2 The CMS detector

The central feature of the CMS detector is a superconducting solenoid of 6 m internal diameter, providing a magnetic field of 3.8 T. Within the field volume, the inner tracker is formed by a silicon pixel and strip tracker. It measures charged particles within the pseudorapidity range $|\eta| < 2.5$. The tracker provides a transverse impact parameter resolution of approximately 15 μm and a resolution on p_T of about 1.5% for 100 GeV particles. Also inside the field volume are a crystal electromagnetic calorimeter, and a brass and scintillator hadron calorimeter. Muons are measured in gas-ionization detectors embedded in the steel flux-return yoke, in the pseudorapidity range $|\eta| < 2.4$, with detector planes made using three technologies: drift tubes, cathode strip chambers, and resistive-plate chambers. Matching muons to tracks measured in the silicon tracker results in a p_T resolution between 1% and 5%, for p_T values up to 1 TeV. Forward calorimetry extends the coverage provided by the barrel and endcap detectors up to $|\eta| < 5$. A detailed description of the CMS detector, together with a definition of the coordinate system used and the relevant kinematic variables, can be found in Ref. [26].

3 Event reconstruction and simulation

A particle-flow algorithm [27, 28] is used to reconstruct and identify all particles in the event, i.e. electrons, muons, photons, charged hadrons, and neutral hadrons, with an optimal combination of all CMS detectors systems.

The reconstructed primary vertex with the largest p_T^2-sum of its associated tracks is chosen as the vertex of the hard interaction and used as reference for the other physics objects.

Jets are clustered from the reconstructed particle candidates using the anti-k_T algorithm [29] with a distance parameter of $R = 0.5$, and each jet is required to pass dedicated quality cri-

teria to suppress the impact of instrumental noise and misreconstruction. Contributions from additional proton-proton interactions within the same bunch crossing (pileup) affect the jet momentum measurement. To mitigate this effect, charged particles associated with other vertices than the reference primary vertex are discarded in the jet reconstruction, and residual contributions (e.g. from neutral particles) are accounted for using a jet-area based correction [30]. Jets originating entirely from pileup interactions are identified and rejected based on vertex and jet-shape information [31]. Jet energy corrections are derived from simulation, and are confirmed with in situ measurements of the energy balance in dijet and Z/γ+jet events [32].

For the offline identification of b jets, the combined secondary vertex (CSV) algorithm [33] is used. This algorithm combines information on track impact parameters and secondary vertices within a jet in a single likelihood discriminant that provides a good separation between b jets and jets of other flavors. Secondary-vertex reconstruction is performed with an inclusive vertex search amongst the tracks associated with a jet [34].

Simulated samples of signal and background events, also referred to as Monte Carlo (MC) samples, were produced using the PYTHIA [35] and MADGRAPH [36] event generators and include pileup events. The response of the CMS detector is modeled with GEANT4 [37]. The MSSM Higgs signal samples, $pp \to b\bar{b}\phi$+X with $\phi \to b\bar{b}$, were produced at leading order in the 4-flavor scheme with PYTHIA version 6.4.12. The p_T and η distributions of the leading associated b jet are in good agreement with the next-to-leading order (NLO) calculations [38]. The multijet background from quantum chromodynamics (QCD) processes has been produced with PYTHIA, while for $t\bar{t}$ +jets events the MADGRAPH event generator was used in its version 5.1.5.11. For all generators, fragmentation, hadronization, and the underlying event have been modeled using PYTHIA with tune Z2*. The most recent PYTHIA 6 Z2* tune is derived from the Z1 tune [39], which uses the CTEQ5L parton distribution functions (PDF) set, whereas Z2* adopts the CTEQ6L [40] PDF set.

4 Trigger and event selection

A major challenge to this analysis is posed by the huge hadronic interaction rate at the LHC, and it is addressed with a dedicated trigger scheme, designed especially to suppress the QCD multijet background. Only events with at least two jets in the pseudorapidity range of $|\eta| \leq 1.74$ are selected. The leading jet (here and in the following the jets are ordered by decreasing p_T) is required to have $p_T > 80\,\text{GeV}$, while the subleading jet must have $p_T > 70\,\text{GeV}$. Furthermore, the event is only accepted if the absolute value of the difference in pseudorapidity between any two jets fulfilling the p_T and η requirements is less than or equal to 1.74. The tight online requirements on the angular variables of the jets are introduced to reduce the trigger rates while preserving the signal significances in the probed mass range of the Higgs bosons. At the trigger level, b jets are identified using an algorithm that requires at least two tracks with high 3D impact parameter significance to be associated with the jet. At least two jets within the event must meet the online b tagging criteria to be accepted by the trigger. The efficiency of the jet-p_T requirements in the trigger are derived from the data with zero-bias triggered events. The online b tagging efficiencies relative to the offline b tagging selection are obtained from simulations of QCD events generated with PYTHIA and scaled to account for the different b tagging efficiencies between data and simulation. The total trigger efficiency for events satisfying the offline selection requirements detailed below ranges from 46–62% over the Higgs boson mass range of 100–900 GeV.

The offline selection requires events to have the two leading jets within $|\eta| \leq 1.65$ to be fully within the pseudorapidity windows of the trigger, and the third leading jet within $|\eta| \leq 2.2$.

The three leading jets must also pass p_T thresholds of 80, 70 and 20 GeV, respectively. In addition, the two leading jets must have a pseudorapidity difference of $|\Delta\eta_{12}| \leq 1.4$, because the QCD multijet background increases significantly with respect to the expected signal with increasing $|\Delta\eta_{12}|$. A minimal pairwise separation of $\Delta R > 1$ between the three leading jets, where $\Delta R = \sqrt{(\Delta\eta)^2 + (\Delta\phi)^2}$ and $\Delta\eta$ and $\Delta\phi$ are the pseudorapidity and azimuthal angle differences (in radians) between the two jets, is imposed to suppress background from b quark pairs arising from gluon splitting.

In the following, "triple-b-tag" and "double-b-tag" samples are introduced, which play crucial roles in the analysis. The triple-b-tag sample is the basis for the signal search. It is defined by requiring all three leading jets to satisfy a tight CSV b tagging selection requirement at a working point characterized by a misidentification probability for light-flavor jets (attributed to u, d, s, or g partons) of about 0.1% at an average jet p_T of 80 GeV. The typical corresponding efficiency for b jets is about 50–60% in the central pseudorapidity region. The total number of events passing the trigger and offline selections is approximately 69 k.

The double-b-tag sample plays a key role in the estimation of the multijet background. In this selection, only two of the three leading jets must pass the tight CSV b tagging requirement. The total number of double-b-tag events remaining after the trigger and offline selections is about 2.4 M. While this definition does not explicitly exclude the triple-b-tag events, the potential signal contribution is negligible due to the size of the QCD multijet background in the double-b-tag sample.

An additional flavor-sensitive quantity, the secondary vertex mass sum of a jet, $\Sigma M_{SV,j}$, is introduced to further improve the separation between jets of different flavor on top of the CSV b tagging requirement. It is defined as the sum of the invariant masses calculated from the tracks forming secondary vertices inside a jet, and thus provides additional separation power. The extension of the signal mass range compared to the previous 7 TeV analysis implies that the jets can have larger p_T, with the consequence that b-tagged jets from background events have a higher probability to contain two heavy flavor quarks instead of at most one. This can occur for example if a very energetic gluon splits into a pair of b or c quarks with a narrow opening angle. For this reason, b and c quark pairs merged into the same jet, labeled as "b2" and "c2", respectively, are treated separately from the cases of unmerged b and c quarks, labeled "b1" and "c1", respectively.

The subsequent analysis will use the secondary vertex mass information to categorize events and to build background templates. Therefore, the secondary vertex mass sums of the three leading jets are combined into a condensed event b tagging estimator, X_{123}. The construction of this estimator is shown in Table 1. Each selected jet j, where j is the rank of the jet in order of decreasing p_T, is assigned an index B_j, which can take one of the four possible integer values from 0–3 according to its secondary vertex mass sum value, as shown in Table 1 (left). For jets with no reconstructed secondary vertex, B_j is also set to zero. The definition of these index regions is motivated by the population of the secondary vertex mass sum by the different jet flavors. From the three indices B_1, B_2, and B_3, a combined event b tagging variable X_{123} is constructed as shown in Table 1 (right). By definition, the event b tagging variable X_{123} can assume nine possible values ranging from 0 to 8. The events are then categorized according to the value of X_{123}, with the rationale of having sufficient statistics in each bin.

Table 1: Left: Definition of the index B_j according to the value of the secondary vertex mass sum of the jet. Right: Definition of the values of the combined event b tagging estimator X_{123} for all combinations of the secondary vertex mass sum indices B_1, B_2, and B_3.

$\Sigma M_{SV,j}$ [GeV]	B_j
0–1	0
1–2	1
2–3	2
>3	3

B_3	$B_1 + B_2$		
	0–1	2–3	4–6
0–1	0	1	2
2	3	4	5
3	6	7	8

5 Background model

The main background for this analysis originates from QCD multijet production, with at least two energetic jets actually containing b hadrons, and a third jet that passes the b tagging selection but possibly as a result of a mistag. Since this type of background cannot be accurately predicted by MC simulation, it is estimated from the data using control samples. The chosen method is similar to the one used in Ref. [41]. The background is modeled by a combination of templates, which are constructed from the double-b-tag sample. Only the shape of these background templates is relevant, since the normalization will be determined by the fit to the data.

Three categories of events are distinguished in the double-b-tag sample, which are denoted as xbb, bxb and bbx depending on whether the jet with the highest, second-highest or third-highest p_T is exempt from the b-tag requirement. In this notation the three jets are referred to in order of decreasing p_T.

From these three double-b-tag categories, background templates are constructed by weighting each untagged jet with the b tagging probability according to its *assumed* flavor. In the template nomenclature, the convention is to indicate the assumed flavor with a capital letter, and it can be one of the five options Q, C1, B1, C2, and B2, where Q refers to light quarks or gluons, while C1 and C2 refer to a jet with a single charm quark and a pair of charm quarks, respectively. Similarly, B1 and B2 refer to jets assumed to contain a single bottom quark and a pair of bottom quarks, respectively. The total number of templates is therefore 15. Each background template is a binned distribution in the two-dimensional space spanned by M_{12}, the dijet mass of the two leading jets, and the event b tagging variable X_{123}. For the construction of each template, each event is weighted with the b tagging probability corresponding to the assumed flavor of the untagged jet. The b tagging probability for each flavor is determined with simulated QCD multijet events, where the flavor selection is based on Monte Carlo truth information. Data/MC scale factors for the b tagging efficiencies are applied where appropriate [33]. Since the b tagging efficiency has a characteristic dependence on p_T and η for each flavor, the weighting results in different shapes of the M_{12} distributions. The X_{123} dimension of the templates is modeled in an analogous fashion. Each of the four possible values of the secondary vertex mass sum index of the untagged jet is taken into account with a weight according to the probability that a jet will end up in a given bin of the secondary vertex mass sum distribution. These probabilities, parametrized as a function of the jet p_T and η, were determined from simulated events, and validated in control data samples.

Two additional corrections are applied to the templates. The first correction addresses a contamination in the double-b-tag sample from non-bb events at the level of a few percent. This contamination is estimated directly from the data using a negative b tagging discriminator [33] constructed with a track counting algorithm based on the negative impact parameter of the tracks, ordered from the most negative impact parameter significance upward. A second cor-

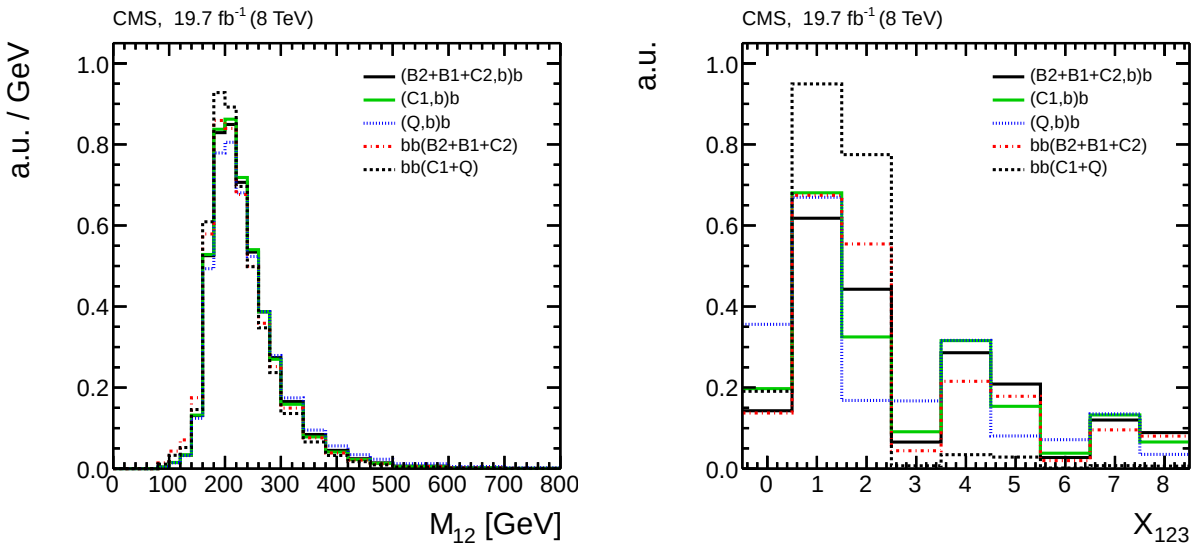

Figure 2: Projections of M_{12} (left) and X_{123} (right) for the five background templates used in the fit. The vertical scale is shown in arbitrary units.

rection is required since the online b tagging patterns are different in the double- and the triple-b-tag samples. In double-b-tag events, the two online b tags usually coincide with the offline b tags, while in triple-b-tag events the online b tags can be assigned to any two-jet subset of the three leading jets. The correction is computed from simulated QCD multijet events, and is applied in the form of additional weights to the events in the double-b-tag sample.

Similarity in shape between some templates leads to unnecessary redundancy. For this reason, similar templates are combined using a χ^2-based metric to guide the decisions. The relative weights in a combination are taken from MC. In the cases where one of the two leading jets is untagged, and the flavor assumption is the same, e.g. Qbb, and bQb, the templates are combined, resulting in a merged template (Q,b)b = Qbb + bQb. By analogy, also (C1,b)b, (B1,b)b, (C2,b)b, and (B2,b)b are obtained. The resulting set of ten templates still shows many similarities. For this reason, (B1,b)b, (B2,b)b, and (C2,b)b are combined into a single template; bbB1, bbB2, and bbC2 into a second; and bbC1 and bbQ into a third. The total number of templates to be fitted in combination to the data is thus reduced to five, namely (B2+B1+C2,b)b, (C1,b)b, (Q,b)b, bb(B2+B1+C2), and bb(C1+Q). The projections of the M_{12} and X_{123} variables are shown in Fig. 2 for these five background templates.

Beyond QCD multijet production, top-quark pair ($t\bar{t}$) events pose the largest potential background to the signal topology. The requirement of three b-tagged jets reduces this background substantially, since only two highly energetic b-tagged jets are expected from the decays of the top quarks. However, one of the W bosons can decay into a $c\bar{s}$ pair, and the c jet can be mistagged as b jet. Using the $t\bar{t}$ Monte Carlo sample, the $t\bar{t}$ contribution is found to be relatively small; the number of $t\bar{t}$ events passing the selections of the double- and triple-b-tag datasets it estimated to be about a factor of 70 smaller than the total amount of data in these samples. The invariant mass spectrum from $t\bar{t}$ is very similar to the one from the QCD multijet background, and does not show any narrow peaks. Since the $t\bar{t}$ events contribute to the double-b-tag sample, they are also taken into account in the background model.

6 Signal modeling

6.1 Signal templates

A signal template is obtained for each MSSM Higgs boson mass considered by applying the full selection to the corresponding simulated signal data set, for nominal masses in the range of 100–900 GeV. The sensitivity of this analysis does not extend down to cross sections as low at that of the SM Higgs boson. Thus, a signal model with a single mass peak is sufficient, in contrast to the $\phi \to \tau\tau$ analysis [14], where the signal model comprises the three neutral Higgs bosons of the MSSM, one of which is SM-like. The projections for the M_{12} and X_{123} distributions

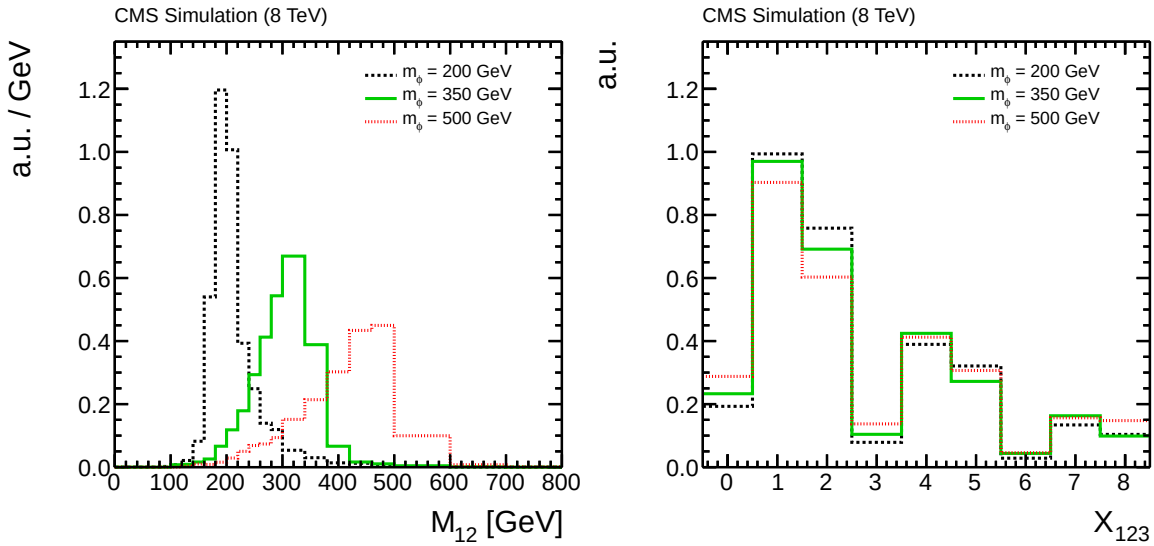

Figure 3: The M_{12} (left) and X_{123} (right) projections of the signal templates for Higgs boson masses of m_ϕ = 200, 350 and 500 GeV. The vertical scale is shown in arbitrary units.

of the signal templates for three different Higgs boson masses are shown in Fig. 3. The shape of the mass distribution is dominated by the experimental resolution and the combinatorial background. The natural width expected for a MSSM Higgs boson in the considered mass and $\tan\beta$ region is negligible in comparison with the detector resolution. At a mass of 500 GeV and $\tan\beta = 50$, for example, the natural width of the mass peak is found to be 13 GeV, which is only ≈14% of the RMS of the reconstructed mass distribution. The X_{123} distributions show little variation with the MSSM Higgs boson mass; they reflect the triple-b-quark signature.

6.2 Signal efficiency

The signal efficiency for each MSSM Higgs mass point is obtained from the simulated data sets. The efficiency of the kinematic trigger selection has been derived with data from control triggers and is applied by weighting. Scale factors to account for the different b tagging efficiencies in data and MC [33] are also applied. The efficiency ranges between 0.17 and 6.38 per mille and peaks around 300 GeV. The detailed mass dependence is shown in Appendix A. The decrease of the efficiency for masses beyond 300 GeV is due to the degradation of the b tagging efficiency at high jet p_T. For masses around 300 GeV the kinematic selections give rise to an efficiency of approximately 0.12, which is reduced to approximately 0.0065 when triple b tagging is required.

6.3 Fitting procedure

The overall two-dimensional distribution in the variables M_{12} and X_{123} is fitted by a model combining the background templates and optionally a signal template. A binned likelihood technique is used. The relative contribution of each template is determined by the fit. The systematic uncertainties are represented by nuisance parameters that are varied in the fit according to their probability density functions.

7 Systematic uncertainties

The following systematic uncertainties in the expected signal and background estimates affect the determination of the signal yield and/or its interpretation within the MSSM.

Uncertainties in the yields of the signal contributions include the uncertainty in the luminosity estimate [42], the statistical uncertainties in the signal MC samples, and the uncertainties of the relative online b tagging corrections. Also taken into account are the QCD renormalization and factorization scale (μ_r, μ_f) uncertainties, the uncertainties due to the parton distribution functions (PDF) and the strong coupling constant α_s, and the uncertainties in the underlying event and parton shower modeling, which all only affect the translation of the signal cross section into $\tan\beta$ in the MSSM interpretation. They have no effect on the signal cross section measurement itself.

The rate as well as the shape of the signal contributions are also affected by the uncertainties in the trigger efficiencies, the jet energy scale, the jet energy resolution, and the pileup modeling, as well as the scale factors for the b-tag efficiency, the mistag rate, and the secondary vertex mass scale. The last three also affect the shapes of the background templates (recall that only the shape is relevant for the background templates). The statistical uncertainty in the template shape, due to the limited size of the double-b-tag sample and due to the uncertainty in the offline b-tag efficiencies and mistag rates, are propagated into the templates and accounted for in the fitting procedure. Additional systematic uncertainties in the shapes of the background-templates arise from the impurity of the double-b-tag sample and the online b tag correction to the templates. The sources and types of systematic uncertainties and their impact on the expected limit are summarized in Table 2.

Table 2: Systematic uncertainties and their relative impact on the expected limit. The values represent an average over the mass range from 100–900 GeV, except for the template statistical and the offline b tagging (bc) uncertainties, where ranges are given.

Source	Type	Target	Impact
Online b tagging	Rate	Signal	11%
Integrated luminosity	Rate	Signal	0.1%
Jet trigger	Rate + Shape	Signal	0.1%
Jet energy scale	Rate + Shape	Signal	0.5%
Jet energy resolution	Rate + Shape	Signal	0.1%
Offline b tagging (bc)	Rate + Shape	Signal + Background	2–16%
Offline b tagging (udsg)	Shape	Background	0.2%
Template stat. uncertainty	Shape	Background	1–21%
Secondary vertex mass sum	Shape	Signal + Background	0.9%
bb purity correction	Shape	Background	3.4%
Online b tagging correction	Shape	Background	0.5%

8 Results

8.1 Background-only fit

In the first step, an unconstrained fit is performed without inclusion of a signal template, involving a linear combination of the background templates only. Results are shown in Fig. 4 and

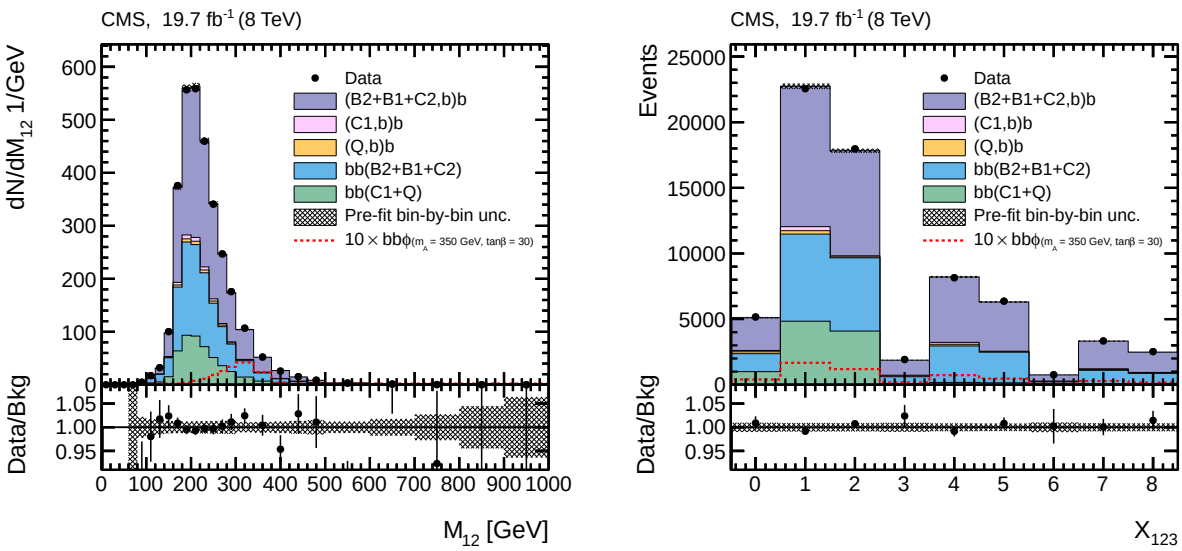

Figure 4: Projections of the dijet mass M_{12} (left) and event b-tag variable X_{123} (right) in the triple-b-tag sample, together with the corresponding projections of the fitted background templates. The hatched area shows the total bin-by-bin background uncertainty of the templates prior to the fit, which takes into account the limited size of the double-b-tag sample and the uncertainties of the offline b-tag efficiencies and mistag rates. For illustration, the signal contribution expected in the $m_{\mathrm{h}}^{\mathrm{max}}$ benchmark scenario of the MSSM with $m_{\mathrm{A}} = 350\,\mathrm{GeV}$, $\tan\beta = 30$, and $\mu = +200\,\mathrm{GeV}$ is overlayed, scaled by a factor 10 for better readability. In addition, the ratio of data to the background estimate is shown at the bottom.

Table 3. There is no indication of a signal. The template-based background model describes the data well within the uncertainty of the template fits with a goodness-of-fit of $\chi^2/N_{\mathrm{dof}} = 207.9/209$, where N_{dof} is the number of degrees of freedom, corresponding to a p-value of 0.51. As expected, the fit is dominated by templates involving triple b-jet signatures, whose fitted total contributions amount to ≈82%.

8.2 Combined fit of signal and background templates

In the second step, a signal template is included together with the background templates in the fit, with the relative fractions of signal and background templates allowed to vary freely. The fit is performed for all considered Higgs boson masses from 100 to 900 GeV. None of the fits shows any significant signal excess. Results for a Higgs boson mass of 350 GeV are shown in Fig. 5 and Table 3. At this mass point, the highest fluctuation in the fitted Higgs boson production cross section is observed, corresponding to a local significance of approximately 1.5 standard deviations. The goodness-of-fit is $\chi^2/N_{\mathrm{dof}} = 205.2/208$, corresponding to a p-value of 0.54.

8.3 Upper limits on cross sections times branching fractions

Cross sections are obtained from the fractions determined by the fit multiplied by the total number of data events after the selection in the signal region, and divided by the corresponding signal efficiencies (Section 6.2) and the integrated luminosity of $19.7\,\mathrm{fb}^{-1}$.

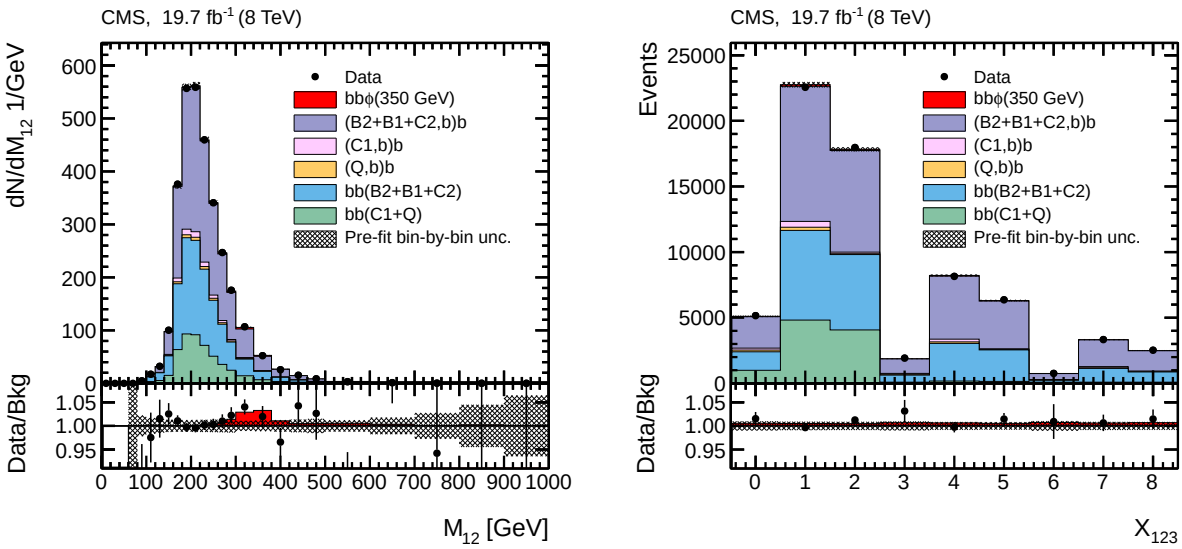

Figure 5: Results from the combined fit of signal and background templates in the triple-b-tag sample, at the 350 GeV mass point. The left plot shows the projections of the dijet mass M_{12}, the right plot the projections of the event b-tag variable X_{123}. The red graph represents the fitted Higgs signal contribution. The hatched area shows the total bin-by-bin background uncertainty of the templates prior to the fit, which takes into account the limited size of the double-b-tag sample and the uncertainties of the offline b-tag efficiencies and mistag rates. In addition, the ratio of data to the background estimate is shown at the bottom.

Table 3: Relative contributions of the individual templates as determined by the background-only and by the signal+background fit for a Higgs boson mass hypothesis of 350 GeV.

Template	Background-only fit fraction [%]	Signal+background fit fraction [%]
(B2+B1+C2,b)b	51.3 ± 3.5	49.5 ± 3.9
(C1,b)b	1.3 ± 2.3	1.7 ± 3.1
(Q,b)b	1.2 ± 2.0	1.1 ± 1.5
bb(B2+B1+C2)	31.2 ± 3.2	32.2 ± 3.4
bb (C1+Q)	15.1 ± 0.9	15.0 ± 0.9
bb$\phi(m = 350\,\text{GeV})$	—	0.5 ± 0.3

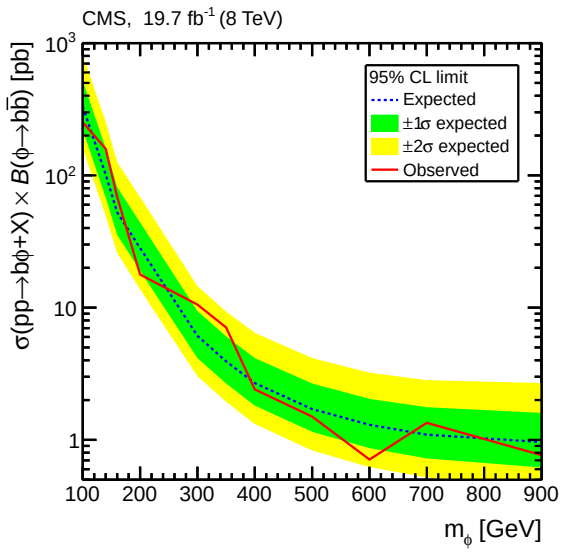

Figure 6: Expected and observed upper limits at 95% CL on $\sigma(\mathrm{pp} \to \mathrm{b}\phi + \mathrm{X})\, \mathcal{B}(\phi \to \mathrm{b}\bar{\mathrm{b}})$ as a function of m_ϕ, where ϕ denotes a generic neutral Higgs-like state.

In the absence of any significant signal, the results are translated into upper limits on the cross section times the branching fraction, $\sigma(\mathrm{pp} \to \mathrm{b}\phi + \mathrm{X})\, \mathcal{B}(\phi \to \mathrm{b}\bar{\mathrm{b}})$, of a generic Higgs-like state in the mass range 100–900 GeV. For calculations of exclusion limits, the modified frequentist construction $\mathrm{CL_s}$[43, 44] is adopted using the ROOSTATS package [45]. The chosen test statistic, used to determine how signal- and background-like the data are, is based on the profile likelihood ratio. Systematic uncertainties are incorporated in the analysis via nuisance parameters and treated as pseudo-observables, following the frequentist paradigm. These uncertainties have been listed in Section 7.

The observed and the median expected 95% confidence level (CL) limits as a function of the Higgs boson mass are shown in Fig. 6 and listed in Table 5 in Appendix B. The 1σ and 2σ bands of the test statistic, including systematic uncertainties, are also shown.

8.4 Interpretation within the MSSM

The cross section limits shown in Fig. 6 are further translated into exclusion limits on the MSSM parameters $\tan\beta$ and m_A. The interpretation is performed using the NNLO cross sections calculated with the BBH@NNLO [46] generator for $\mathrm{b} + \mathrm{h/H/A}$ associated production in the Santander matching of the 4-flavor and 5-flavor schemes [47] and the branching fractions computed with the FEYNHIGGS program [48–51].

The observed and expected 95% CL median upper limits on $\tan\beta$ versus m_A, together with the 1σ and 2σ bands, are shown in Fig. 7 (left). They have been computed within the traditional MSSM $m_\mathrm{h}^\mathrm{max}$ benchmark scenario [52] with the higgsino mass parameter $\mu = +200$ GeV. The observed upper limits range from $\tan\beta$ about 20 in the low-m_A region to about 50 at $m_\mathrm{A} = 500$ GeV, and extend the existing measurement at 7 TeV [25] into the hitherto unexplored m_A region beyond 350 GeV. The model interpretation is not extended to higher masses above 500 GeV because the theoretical predictions are not reliable for $\tan\beta$ much higher than 60.

While the cross section limits obtained from the 2011 and 2012 data cannot be combined directly due to the different center-of-mass energies, such a combination is possible for the model-dependent interpretation. The resulting upper limits on $\tan\beta$ versus m_A from both data periods are shown in Figure 7 (right). While the sensitivity is significantly enhanced compared to the

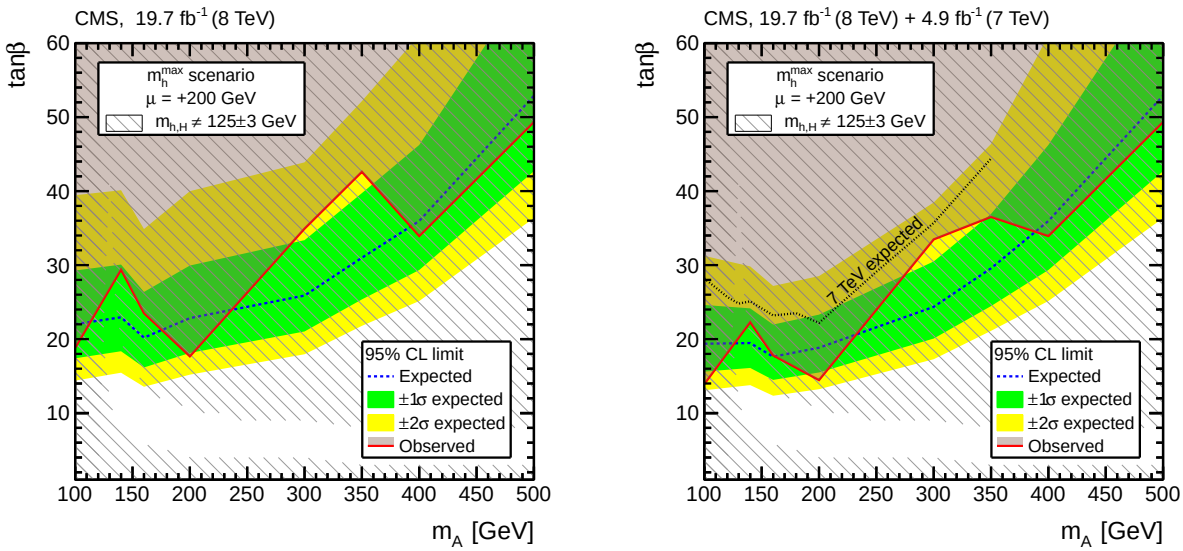

Figure 7: Expected and observed upper limits at 95% CL for the MSSM parameter $\tan\beta$ versus m_A in the m_h^{max} benchmark scenario with $\mu = +200$ GeV. The excluded parameter space (observed limit) is indicated by the shaded area. Regions where the mass of neither of the CP-even MSSM Higgs bosons h or H is compatible with the discovered Higgs boson of 125 GeV within a range of 3 GeV are marked by the hatched areas. The left plot shows the result obtained with the 8 TeV data only, the right plot shows the result obtained after a combination with the 7 TeV data. For comparison, the expected limit of the 7 TeV data analysis [25] is overlayed.

7 TeV analysis [25] already up to 350 GeV, the addition of the 7 TeV result visibly improves the sensitivity in the low-mass area below 200 GeV. The observed limit for $\tan\beta$ ranges down to about 14 at the lowest m_A value considered.

Association of one of the CP-even MSSM Higgs bosons h and H with the measured state at a mass of 125 GeV within a margin of ± 3 GeV that reflects the theoretical uncertainties [20] leads to an indirect constraint on $\tan\beta$. The incompatible regions in the parameter space are illustrated by the hatched areas in both plots in Fig. 7. In the m_h^{max} scenario, the MSSM parameters beyond tree level have been tuned such that m_h becomes as large as possible. As a result, large m_A and already moderate values of $\tan\beta$ lead to m_h values that are higher than the measured Higgs boson mass. This apparent exclusion of large $\tan\beta$ values is, however, an artificial consequence of the assumptions in the m_h^{max} scenario. Recently, several new MSSM benchmark scenarios have been proposed, which are more naturally compatible with the observed Higgs boson at 125 GeV [20], and among them the m_h^{mod+}, m_h^{mod-}, light-stop, and light-stau scenarios are also used in the following for the interpretation of the results of this analysis. The observed and expected 95% CL exclusion limits in these scenarios with $\mu = +200$ GeV, obtained with the combined 7 and 8 TeV data, are shown in Fig. 8. (The term "stop" refers to the supersymmetric partner of the top quark throughout this paper. Results for the τ-phobic and low-m_H scenarios are not shown because the analysis has sensitivity in a limited mass region only.) The limits obtained in all MSSM benchmark scenarios are listed in Tables 6 to 11 in Appendix B.

The aforementioned sensitivity of the $\phi \to b\bar{b}$ channel to the higgsino mass parameter μ is evident in Fig. 9, where the limit in the m_h^{mod+} scenario is compared for different values of μ. The dependence is particularly pronounced at higher m_A; for example, the observed upper limit on $\tan\beta$ varies from 30 for $\mu = -500$ GeV to beyond 60 for $\mu = +500$ GeV for $m_A = 500$ GeV. The limits are also listed in Table 12 in Appendix B.

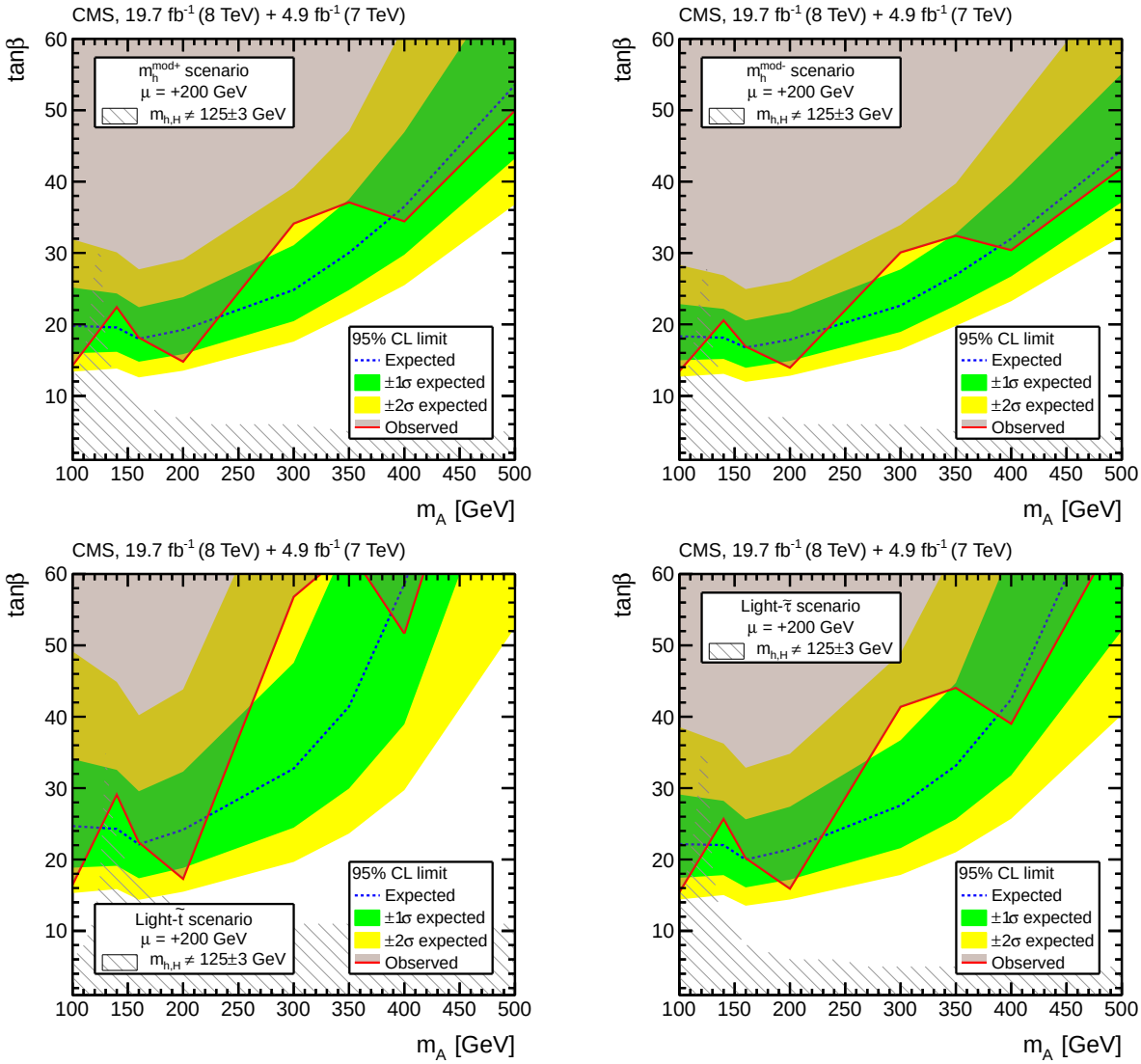

Figure 8: Expected and observed upper limits at 95% CL for the MSSM parameter $\tan\beta$ versus m_A in the m_h^{mod+}, m_h^{mod-}, light-stop, and light-stau benchmark scenarios with $\mu = +200$ GeV [20].

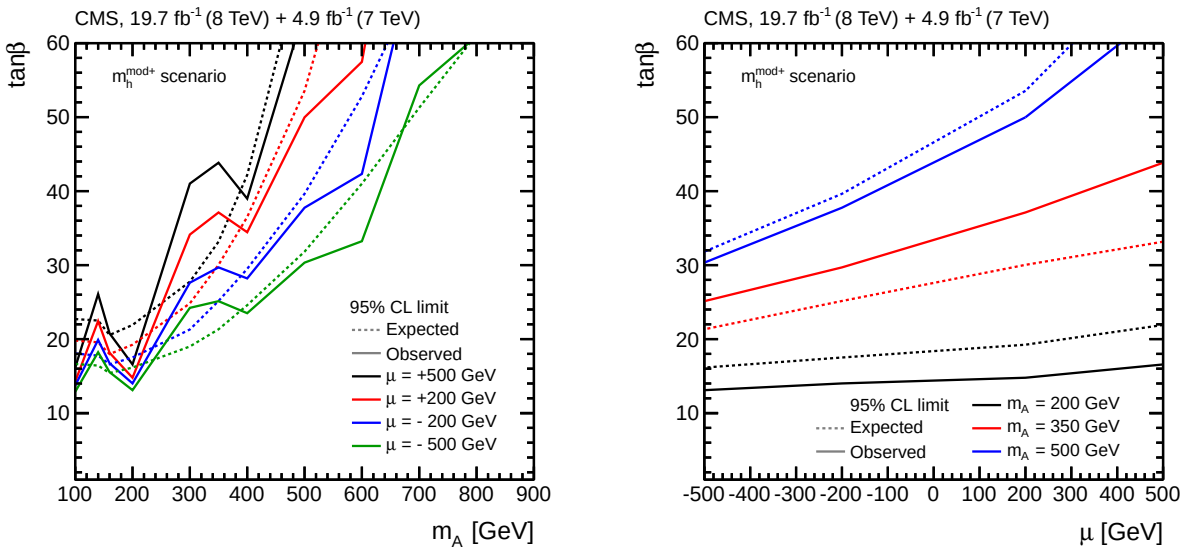

Figure 9: Expected and observed upper limits at 95% CL for the MSSM parameter $\tan\beta$ versus m_{A} for four different values of the higgsino mass parameter μ (left) and versus μ for three different values of m_{A} (right) in the $m_{\mathrm{h}}^{\mathrm{mod+}}$ scenario.

9 Summary

A search for a Higgs boson decaying into a pair of b quarks and accompanied by at least one additional b quark has been performed in proton-proton collisions at a center-of-mass energy of 8 TeV at the LHC, corresponding to an integrated luminosity of 19.7 fb^{-1}. The data were taken with dedicated triggers using all-hadronic jet signatures combined with online b tagging. A selection of events with three b-tagged jets has been performed in the offline analysis. A signal has been searched for in the two-dimensional spectrum formed by the invariant mass of the two leading jets and a condensed event b-tag estimator.

No evidence for a signal is found. The observed distributions are well described by a background model constructed from events in which only two of the three leading jets are required to be b tagged. Upper limits on the Higgs boson cross section times branching fraction are obtained in the mass region from 100–900 GeV, thus extending the search to considerably higher masses than those accessed by the previous 7 TeV analysis. The upper limits range from about 250 pb at the lower end of the mass range, to about 1 pb at 900 GeV.

The results are interpreted within the MSSM in the benchmark scenarios $m_{\mathrm{h}}^{\mathrm{max}}$, $m_{\mathrm{h}}^{\mathrm{mod+}}$, $m_{\mathrm{h}}^{\mathrm{mod-}}$, light-stau and light-stop, and lead to upper limits for the model parameter $\tan\beta$ as a function of the mass parameter m_{A}. In combination with the 7 TeV data, the observed limit for $\tan\beta$ ranges down to about 14 at the lowest m_{A} value of 100 GeV in the $m_{\mathrm{h}}^{\mathrm{mod+}}$ scenario with a higgsino mass parameter of $\mu = +200$ GeV. The limit depends significantly on μ, varying from $\tan\beta = 30$ for $\mu = -500$ GeV to beyond 60 for $\mu = +500$ GeV at $m_{\mathrm{A}} = 500$ GeV.

Acknowledgments

We congratulate our colleagues in the CERN accelerator departments for the excellent performance of the LHC and thank the technical and administrative staffs at CERN and at other CMS institutes for their contributions to the success of the CMS effort. In addition, we gratefully acknowledge the computing centers and personnel of the Worldwide LHC Computing Grid for delivering so effectively the computing infrastructure essential to our analyses. Finally, we

acknowledge the enduring support for the construction and operation of the LHC and the CMS detector provided by the following funding agencies: BMWFW and FWF (Austria); FNRS and FWO (Belgium); CNPq, CAPES, FAPERJ, and FAPESP (Brazil); MES (Bulgaria); CERN; CAS, MoST, and NSFC (China); COLCIENCIAS (Colombia); MSES and CSF (Croatia); RPF (Cyprus); MoER, ERC IUT and ERDF (Estonia); Academy of Finland, MEC, and HIP (Finland); CEA and CNRS/IN2P3 (France); BMBF, DFG, and HGF (Germany); GSRT (Greece); OTKA and NIH (Hungary); DAE and DST (India); IPM (Iran); SFI (Ireland); INFN (Italy); MSIP and NRF (Republic of Korea); LAS (Lithuania); MOE and UM (Malaysia); CINVESTAV, CONACYT, SEP, and UASLP-FAI (Mexico); MBIE (New Zealand); PAEC (Pakistan); MSHE and NSC (Poland); FCT (Portugal); JINR (Dubna); MON, RosAtom, RAS and RFBR (Russia); MESTD (Serbia); SEIDI and CPAN (Spain); Swiss Funding Agencies (Switzerland); MST (Taipei); ThEPCenter, IPST, STAR and NSTDA (Thailand); TUBITAK and TAEK (Turkey); NASU and SFFR (Ukraine); STFC (United Kingdom); DOE and NSF (USA).

Individuals have received support from the Marie-Curie program and the European Research Council and EPLANET (European Union); the Leventis Foundation; the A. P. Sloan Foundation; the Alexander von Humboldt Foundation; the Belgian Federal Science Policy Office; the Fonds pour la Formation à la Recherche dans l'Industrie et dans l'Agriculture (FRIA-Belgium); the Agentschap voor Innovatie door Wetenschap en Technologie (IWT-Belgium); the Ministry of Education, Youth and Sports (MEYS) of the Czech Republic; the Council of Science and Industrial Research, India; the HOMING PLUS program of the Foundation for Polish Science, cofinanced from European Union, Regional Development Fund; the Compagnia di San Paolo (Torino); the Consorzio per la Fisica (Trieste); MIUR project 20108T4XTM (Italy); the Thalis and Aristeia programs cofinanced by EU-ESF and the Greek NSRF; the National Priorities Research Program by Qatar National Research Fund; and Rachadapisek Sompot Fund for Postdoctoral Fellowship, Chulalongkorn University (Thailand).

References

[1] ATLAS Collaboration, "Observation of a new particle in the search for the Standard Model Higgs boson with the ATLAS detector at the LHC", *Phys. Lett. B* **716** (2012) 1, doi:10.1016/j.physletb.2012.08.020, arXiv:1207.7214.

[2] CMS Collaboration, "Observation of a new boson at a mass of 125 GeV with the CMS experiment at the LHC", *Phys. Lett. B* **716** (2012) 30, doi:10.1016/j.physletb.2012.08.021, arXiv:1207.7235.

[3] CMS Collaboration, "Observation of a new boson with mass near 125 GeV in pp collisions at $\sqrt{s}$ = 7 and 8 TeV", *JHEP* **06** (2013) 081, doi:10.1007/JHEP06(2013)081, arXiv:1303.4571.

[4] J. Wess and B. Zumino, "Supergauge transformations in four dimensions", *Nuclear Physics B* **70** (1974) 39, doi:10.1016/0550-3213(74)90355-1.

[5] H. P. Nilles, "Supersymmetry, supergravity and particle physics", *Phys. Rept.* **110** (1984) 1, doi:10.1016/0370-1573(84)90008-5.

[6] S. P. Martin, "A Supersymmetry Primer", (1997). arXiv:hep-ph/9709356.

[7] D. J. H. Chung et al., "The soft supersymmetry breaking Lagrangian: theory and applications", *Phys. Rept.* **407** (2005) 1, doi:10.1016/j.physrep.2004.08.032, arXiv:hep-ph/0312378.

[8] G. Bertone, D. Hooper, and J. Silk, "Particle dark matter: evidence, candidates and constraints", *Phys. Rept.* **405** (2005) 279, doi:10.1016/j.physrep.2004.08.031.

[9] S. Dimopoulos, S. Raby, and F. Wilczek, "Supersymmetry and the scale of unification", *Phys. Rev. D* **24** (1981) 1681, doi:10.1103/PhysRevD.24.1681.

[10] E. Witten, "Mass hierarchies in supersymmetric theories", *Phys. Lett. B* **105** (1981) 267, doi:10.1016/0370-2693(81)90885-6.

[11] LHC Higgs Cross Section Working Group, "Handbook of LHC Higgs Cross Sections: 3. Higgs Properties", CERN Report CERN-2013-004, FERMILAB-CONF-13-667-T, 2013. doi:10.5170/CERN-2013-004, arXiv:1307.1347.

[12] CMS Collaboration, "Search for neutral Higgs bosons decaying to tau pairs in pp collisions at $\sqrt{s} = 7$ TeV", *Phys. Lett. B* **713** (2012) 68, doi:10.1016/j.physletb.2012.05.028, arXiv:1202.4083.

[13] ATLAS Collaboration, "Search for the neutral Higgs bosons of the minimal supersymmetric standard model in pp collisions at $\sqrt{s} = 7$ TeV with the ATLAS detector", *JHEP* **02** (2013) 095, doi:10.1007/JHEP02(2013)095, arXiv:1211.6956.

[14] CMS Collaboration, "Search for neutral MSSM Higgs bosons decaying to a pair of tau leptons in pp collisions", *JHEP* **10** (2014) 160, doi:10.1007/JHEP10(2014)160, arXiv:1408.3316.

[15] ATLAS Collaboration, "Search for neutral Higgs bosons of the minimal supersymmetric standard model in pp collisions at $\sqrt{s}$ = 8 TeV with the ATLAS detector", *JHEP* **11** (2014) 056, doi:10.1007/JHEP11(2014)056, arXiv:1409.6064.

[16] ALEPH, DELPHI, L3, and OPAL Collaborations, LEP Working Group for Higgs Boson Searches, "Search for neutral MSSM Higgs bosons at LEP", *Eur. Phys. J. C* **47** (2006) 547, doi:10.1140/epjc/s2006-02569-7, arXiv:hep-ex/0602042.

[17] CDF Collaboration, "Search for Higgs Bosons Predicted in Two-Higgs-Doublet Models via Decays to Tau Lepton Pairs in 1.96 TeV $p\overline{p}$ Collisions", *Phys. Rev. Lett.* **103** (2009) 201801, doi:10.1103/PhysRevLett.103.201801, arXiv:0906.1014.

[18] D0 Collaboration, "Search for Higgs Bosons Decaying to Tau Pairs in $p\bar{p}$ Collisions with the D0 Detector", *Phys. Rev. Lett.* **101** (2008) 071804, doi:10.1103/PhysRevLett.101.071804, arXiv:0805.2491.

[19] D0 Collaboration, "Search for Higgs bosons of the minimal supersymmetric standard model $p\bar{p}$ in collisions at $\sqrt{s} = 1.96$ TeV", *Phys. Lett. B* **710** (2012) 569, doi:10.1016/j.physletb.2012.03.021, arXiv:1112.5431.

[20] M. Carena et al., "MSSM Higgs boson searches at the LHC: benchmark scenarios after the discovery of a Higgs-like particle", *Eur. Phys. J. C* **73** (2013) 2552, doi:10.1140/epjc/s10052-013-2552-1, arXiv:1302.7033.

[21] G. C. Branco et al., "Theory and phenomenology of two-Higgs-doublet models", *Phys. Rep.* **516** (2012) 1, doi:10.1016/j.physrep.2012.02.002, arXiv:1106.0034.

[22] E. Izaguirre, G. Krnjaic, and B. Shuve, "Bottom-up approach to the Galactic Center excess", *Phys. Rev. D* **90** (2014) 055002, doi:10.1103/PhysRevD.90.055002, arXiv:1404.2018.

[23] A. Berlin, D. Hooper, and S. D. McDermott, "Simplified dark matter models for the Galactic Center gamma-ray excess", *Phys. Rev. D* **89** (2014) 115022, doi:10.1103/PhysRevD.89.115022, arXiv:1404.0022.

[24] CDF and D0 Collaborations, "Search for neutral Higgs bosons in events with multiple bottom quarks at the Tevatron", *Phys. Rev. D* **86** (2012) 091101, doi:10.1103/PhysRevD.86.091101, arXiv:1207.2757.

[25] CMS Collaboration, "Search for a Higgs boson decaying into a b-quark pair and produced in association with b quarks in proton-proton collisions at 7 TeV", *Phys. Lett. B* **722** (2013) 207, doi:10.1016/j.physletb.2013.04.017, arXiv:1302.2892.

[26] CMS Collaboration, "The CMS experiment at the CERN LHC", *JINST* **3** (2008) S08004, doi:10.1088/1748-0221/3/08/S08004.

[27] CMS Collaboration, "Particle-flow event reconstruction in CMS and performance for jets, taus, and $E_{\mathrm{T}}^{\mathrm{miss}}$", CMS Physics Analysis Summary CMS-PAS-PFT-09-001, 2009.

[28] CMS Collaboration, "Commissioning of the particle-flow event reconstruction with the first LHC collisions recorded in the CMS detector", CMS Physics Analysis Summary CMS-PAS-PFT-10-001, 2010.

[29] M. Cacciari, G. P. Salam, and G. Soyez, "The anti-k_t jet clustering algorithm", *JHEP* **04** (2008) 063, doi:10.1088/1126-6708/2008/04/063, arXiv:0802.1189.

[30] M. Cacciari and G. P. Salam, "Pileup subtraction using jet areas", *Phys. Lett. B* **659** (2008) 119, doi:10.1016/j.physletb.2007.09.077, arXiv:0707.1378.

[31] CMS Collaboration, "Pileup Jet Identification", CMS Physics Analysis Summary CMS-PAS-JME-13-005, 2013.

[32] CMS Collaboration, "Determination of Jet Energy Calibration and Transverse Momentum Resolution in CMS", *JINST* **6** (2011) P11002, doi:10.1088/1748-0221/6/11/P11002, arXiv:1107.4277.

[33] CMS Collaboration, "Identification of b-quark jets with the CMS experiment", *JINST* **8** (2013) P04013, doi:10.1088/1748-0221/8/04/P04013, arXiv:1211.4462.

[34] W. Waltenberger, "Adaptive Vertex Reconstruction", CMS NOTE 2008-033, 2008.

[35] T. Sjöstrand, S. Mrenna, and P. Z. Skands, "PYTHIA 6.4 physics and manual", *JHEP* **05** (2006) 026, doi:10.1088/1126-6708/2006/05/026, arXiv:hep-ph/0603175.

[36] J. Alwall et al., "MadGraph 5: going beyond", *JHEP* **06** (2011) 128, doi:10.1007/JHEP06(2011)128, arXiv:1106.0522.

[37] GEANT4 Collaboration, "GEANT4: a simulation toolkit", *Nucl. Instrum. Meth. A* **506** (2003) 250, doi:10.1016/S0168-9002(03)01368-8.

[38] LHC Higgs Cross Section Working Group, S. Dittmaier et al., "Handbook of LHC Higgs Cross Sections: 2. Differential Distributions", CERN Report CERN-2012-002, 2012. doi:10.5170/CERN-2012-002, arXiv:1201.3084.

[39] R. Field, "Early LHC Underlying Event Data - Findings and Surprises", (2010). arXiv:1010.3558.

[40] J. Pumplin et al., "New Generation of Parton Distributions with Uncertainties from Global QCD Analysis", *JHEP* **07** (2002) 12, doi:10.1088/1126-6708/2002/07/012, arXiv:hep-ph/0201195.

[41] CDF Collaboration, "Search for Higgs bosons produced in association with b quarks", *Phys. Rev. D* **85** (2012) 032005, doi:10.1103/PhysRevD.85.032005, arXiv:1106.4782.

[42] CMS Collaboration, "CMS Luminosity Based on Pixel Cluster Counting - Summer 2013 Update", CMS Physics Analysis Summary CMS-PAS-LUM-13-001, 2013.

[43] T. Junk, "Confidence level computation for combining searches with small statistics", *Nucl. Instrum. Meth. A* **434** (1999) 435, doi:10.1016/S0168-9002(99)00498-2, arXiv:hep-ex/9902006.

[44] A. L. Read, "Presentation of search results: The CL_s technique", *J. Phys. G* **28** (2002) 2693, doi:10.1088/0954-3899/28/10/313.

[45] L. Moneta et al., "The RooStats Project", in *13th International Workshop on Advanced Computing and Analysis Techniques in Physics Research (ACAT2010)*. SISSA, 2010. arXiv:1009.1003.

[46] R. V. Harlander and W. B. Kilgore, "Higgs boson production in bottom quark fusion at next-to-next-to leading order", *Phys. Rev. D* **68** (2003) 013001, doi:10.1103/PhysRevD.68.013001, arXiv:hep-ph/0304035.

[47] R. Harlander, M. Krämer, and M. Schumacher, "Bottom-quark associated Higgs-boson production: reconciling the four- and five-flavour scheme approach", (2011). arXiv:1112.3478.

[48] G. Degrassi et al., "Towards high-precision predictions for the MSSM Higgs sector", *Eur. Phys. J. C* **28** (2003) 133, doi:10.1140/epjc/s2003-01152-2, arXiv:hep-ph/0212020.

[49] M. Frank et al., "The Higgs boson masses and mixings of the complex MSSM in the Feynman-diagrammatic approach", *JHEP* **02** (2007) 047, doi:10.1088/1126-6708/2007/02/047, arXiv:hep-ph/0611326.

[50] S. Heinemeyer, W. Hollik, and G. Weiglein, "FeynHiggs: A program for the calculation of the masses of the neutral CP even Higgs bosons in the MSSM", *Comput. Phys. Commun.* **124** (2000) 76, doi:10.1016/S0010-4655(99)00364-1, arXiv:hep-ph/9812320.

[51] S. Heinemeyer, W. Hollik, and G. Weiglein, "The masses of the neutral CP-even Higgs bosons in the MSSM: Accurate analysis at the two loop level", *Eur. Phys. J. C* **9** (1999) 343, doi:10.1007/s100529900006, arXiv:hep-ph/9812472.

[52] M. S. Carena, S. Heinemeyer, C. E. M. Wagner, and G. Weiglein, "MSSM Higgs boson searches at the Tevatron and the LHC: Impact of different benchmark scenarios", *Eur. Phys. J. C* **45** (2006) 797, doi:10.1140/epjc/s2005-02470-y, arXiv:hep-ph/0511023.

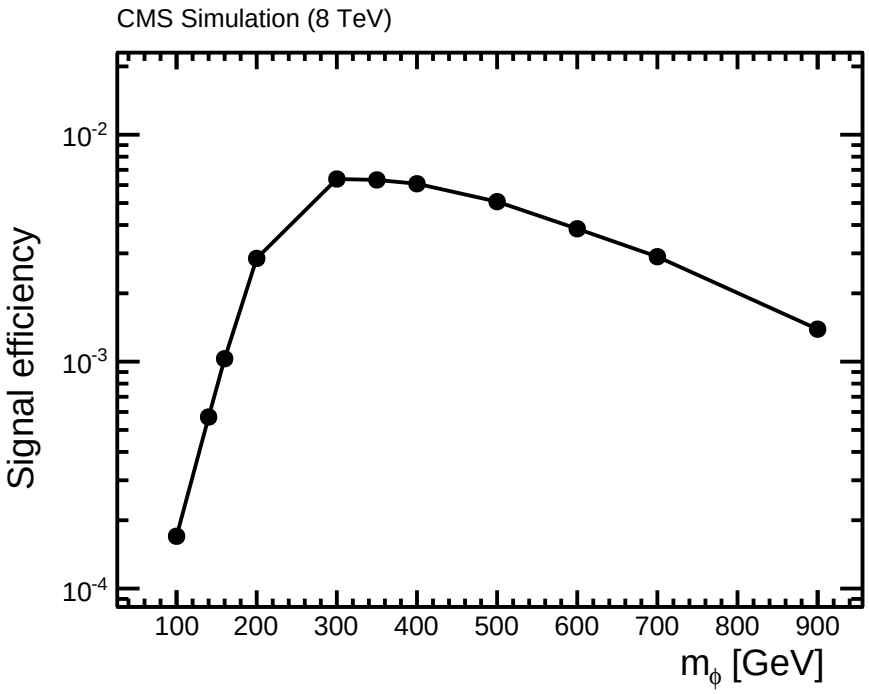

Figure 10: The signal efficiency as a function of the Higgs boson mass m_ϕ, for a center-of-mass energy of 8 TeV.

Appendix A Signal Efficiency

The signal efficiencies are summarized in Table 4 and shown in Fig. 10 as a function of the Higgs boson mass.

Table 4: The total signal efficiency in per mille as a function of the Higgs boson mass m_ϕ, for a center-of-mass energy of 8 TeV.

m_ϕ [GeV]	Efficiency [per mille]
100	0.17
140	0.57
160	1.03
200	2.85
300	6.38
350	6.32
400	6.08
500	5.07
600	3.85
700	2.90
900	1.39

Appendix B Exclusion limits

The model-independent 95% CL limits on $\sigma(\mathrm{pp} \to \mathrm{b}\phi + \mathrm{X})\,\mathcal{B}(\phi \to \mathrm{b}\bar{\mathrm{b}})$ are listed in Table 5 for different Higgs boson masses m_ϕ. The 95% CL limits of $(\tan\beta, m_\mathrm{A})$ are listed in Tables 6 to 11 for different MSSM benchmark scenarios with $\mu = +200\,\mathrm{GeV}$ and for different values of μ in the $m_\mathrm{h}^{\mathrm{mod+}}$ scenario in Table 12.

Table 5: Expected and observed 95% CL upper limits on $\sigma(\mathrm{pp} \to \mathrm{b}\phi + \mathrm{X})\,\mathcal{B}(\phi \to \mathrm{b}\bar{\mathrm{b}})$ in pb as a function of m_ϕ, where ϕ denotes a generic Higgs-like state, as obtained from the 8 TeV data.

Mass [GeV]	-2σ	-1σ	Median	$+1\sigma$	$+2\sigma$	Observed
100	160.7	221.0	330.4	518.8	811.2	251.9
140	49.4	68.0	101.6	161.2	254.7	158.8
160	25.9	35.6	52.5	81.6	126.1	68.7
200	13.7	19.0	28.2	44.1	68.6	17.8
300	3.0	4.1	6.1	9.4	14.5	10.5
350	1.9	2.7	3.9	6.1	9.3	7.1
400	1.3	1.8	2.7	4.2	6.4	2.4
500	0.8	1.2	1.7	2.7	4.2	1.5
600	0.6	0.9	1.3	2.0	3.2	0.7
700	0.5	0.7	1.1	1.8	2.8	1.3
900	0.4	0.6	1.0	1.6	2.7	0.8

Table 6: Expected and observed 95% CL upper limits on $\tan\beta$ as a function of m_A in the $m_\mathrm{h}^{\mathrm{max}}$, $\mu = +200$ GeV, benchmark scenario obtained from the 8 TeV data only.

Mass [GeV]	-2σ	-1σ	Median	$+1\sigma$	$+2\sigma$	Observed
100	14.4	17.4	22.0	29.3	39.4	18.8
140	15.5	18.4	22.9	30.1	40.1	29.4
160	13.6	16.2	20.2	26.4	34.9	23.5
200	15.2	18.1	22.8	29.9	40.0	17.7
300	18.0	21.0	25.9	33.4	43.9	34.9
350	21.8	25.4	31.0	39.7	52.2	42.6
400	25.1	29.3	36.0	46.2	—	33.9
500	36.4	42.7	52.9	—	—	49.4

Table 7: Expected and observed 95% CL upper limits on $\tan\beta$ as a function of m_A in the $m_\mathrm{h}^{\mathrm{max}}$, $\mu = +200$ GeV, benchmark scenario obtained from a combination of the 7 and 8 TeV data.

Mass [GeV]	-2σ	-1σ	Median	$+1\sigma$	$+2\sigma$	Observed
100	13.1	15.6	19.4	24.6	31.2	13.9
140	13.8	16.1	19.5	24.2	29.8	22.3
160	12.3	14.5	17.6	22.0	27.2	17.8
200	13.2	15.5	18.8	23.3	28.5	14.5
300	17.3	20.1	24.4	30.5	38.5	33.5
350	21.1	24.5	29.6	36.9	46.4	36.5
400	25.1	29.3	36.0	46.2	—	33.9
500	36.4	42.7	52.9	—	—	49.4

Table 8: Expected and observed 95% CL upper limits on $\tan\beta$ as a function of m_A in the m_h^{mod+}, $\mu = +200$ GeV, benchmark scenario obtained from a combination of the 7 and 8 TeV data.

Mass [GeV]	-2σ	-1σ	Median	$+1\sigma$	$+2\sigma$	Observed
100	13.4	16.0	19.8	25.1	31.9	14.2
140	13.8	16.2	19.6	24.3	30.1	22.4
160	12.6	14.8	18.0	22.4	27.7	18.2
200	13.5	15.8	19.2	23.8	29.1	14.8
300	17.6	20.5	24.8	31.1	39.2	34.1
350	21.4	24.8	30.0	37.5	47.1	37.1
400	25.5	29.8	36.5	46.9	—	34.4
500	36.8	43.2	53.5	—	—	50.0

Table 9: Expected and observed 95% CL upper limits on $\tan\beta$ as a function of m_A in the m_h^{mod-}, $\mu = +200$ GeV, benchmark scenario obtained from a combination of the 7 and 8 TeV data.

Mass [GeV]	-2σ	-1σ	Median	$+1\sigma$	$+2\sigma$	Observed
100	12.7	15.0	18.3	22.8	28.3	13.4
140	13.1	15.2	18.1	22.2	26.9	20.6
160	11.9	13.9	16.7	20.5	24.9	16.9
200	12.8	14.9	17.9	21.7	26.1	13.9
300	16.5	18.9	22.6	27.7	33.9	30.1
350	19.8	22.7	26.9	32.7	39.7	32.4
400	23.2	26.7	32.0	39.7	49.7	30.4
500	32.3	37.1	44.4	55.1	—	41.9

Table 10: Expected and observed 95% CL upper limits on $\tan\beta$ as a function of m_A in the light-stau, $\mu = +200$ GeV, benchmark scenario obtained from a combination of the 7 and 8 TeV data.

Mass [GeV]	-2σ	-1σ	Median	$+1\sigma$	$+2\sigma$	Observed
100	14.4	17.4	22.2	29.1	38.6	15.4
140	15.0	17.8	22.0	28.2	36.2	25.7
160	13.5	16.1	20.0	25.6	32.9	20.2
200	14.4	17.2	21.4	27.4	34.8	15.9
300	17.8	21.6	27.6	36.7	48.9	41.4
350	21.0	25.7	33.1	44.8	—	44.1
400	25.7	31.8	42.4	—	—	39.0
500	40.3	52.1	—	—	—	—

Table 11: Expected and observed 95% CL upper limits on $\tan\beta$ as a function of m_A in the light-stop, $\mu = +200$ GeV, benchmark scenario obtained from a combination of the 7 and 8 TeV data.

Mass [GeV]	-2σ	-1σ	Median	$+1\sigma$	$+2\sigma$	Observed
100	15.3	18.9	24.7	34.1	49.2	16.5
140	15.9	19.1	24.3	32.6	44.9	29.1
160	14.4	17.4	22.1	29.6	40.2	22.4
200	15.5	18.8	24.2	32.3	43.8	17.3
300	19.7	24.5	32.7	47.6	—	56.8
350	23.6	29.9	41.4	—	—	—
400	29.7	39.0	58.6	—	—	51.7
500	52.5	—	—	—	—	—

Table 12: Observed (expected) 95% CL upper limits on $\tan\beta$ as a function of m_{A} in the $m_{\mathrm{h}}^{\mathrm{mod+}}$ benchmark scenario for different values of the higgsino mass parameter μ obtained from a combination of the 7 and 8 TeV data.

Mass [GeV]	$\mu = -500$ GeV	$\mu = -200$ GeV	$\mu = +200$ GeV	$\mu = +500$ GeV
100	12.9 (16.6)	13.7 (18.1)	14.2 (19.8)	16.1 (22.7)
140	18.2 (16.4)	19.9 (17.8)	22.4 (19.6)	26.1 (22.5)
160	15.5 (15.4)	16.7 (16.6)	18.2 (18.0)	20.8 (20.6)
200	13.1 (16.2)	14.0 (17.5)	14.8 (19.2)	16.6 (21.9)
300	24.2 (19.0)	27.6 (21.3)	34.1 (24.8)	41.0 (27.8)
350	25.1 (21.3)	29.7 (25.1)	37.1 (30.0)	43.8 (33.2)
400	23.5 (24.6)	28.2 (29.5)	34.4 (36.5)	39.0 (42.2)
500	30.3 (31.8)	37.8 (39.6)	50.0 (53.5)	— (—)
600	33.2 (41.0)	42.3 (52.8)	57.5 (—)	— (—)
700	54.3 (51.3)	— (—)	— (—)	— (—)

Appendix C The CMS Collaboration

Yerevan Physics Institute, Yerevan, Armenia
V. Khachatryan, A.M. Sirunyan, A. Tumasyan

Institut für Hochenergiephysik der OeAW, Wien, Austria
W. Adam, E. Asilar, T. Bergauer, J. Brandstetter, E. Brondolin, M. Dragicevic, J. Erö, M. Flechl, M. Friedl, R. Frühwirth[1], V.M. Ghete, C. Hartl, N. Hörmann, J. Hrubec, M. Jeitler[1], V. Knünz, A. König, M. Krammer[1], I. Krätschmer, D. Liko, T. Matsushita, I. Mikulec, D. Rabady[2], B. Rahbaran, H. Rohringer, J. Schieck[1], R. Schöfbeck, J. Strauss, W. Treberer-Treberspurg, W. Waltenberger, C.-E. Wulz[1]

National Centre for Particle and High Energy Physics, Minsk, Belarus
V. Mossolov, N. Shumeiko, J. Suarez Gonzalez

Universiteit Antwerpen, Antwerpen, Belgium
S. Alderweireldt, T. Cornelis, E.A. De Wolf, X. Janssen, A. Knutsson, J. Lauwers, S. Luyckx, S. Ochesanu, R. Rougny, M. Van De Klundert, H. Van Haevermaet, P. Van Mechelen, N. Van Remortel, A. Van Spilbeeck

Vrije Universiteit Brussel, Brussel, Belgium
S. Abu Zeid, F. Blekman, J. D'Hondt, N. Daci, I. De Bruyn, K. Deroover, N. Heracleous, J. Keaveney, S. Lowette, L. Moreels, A. Olbrechts, Q. Python, D. Strom, S. Tavernier, W. Van Doninck, P. Van Mulders, G.P. Van Onsem, I. Van Parijs

Université Libre de Bruxelles, Bruxelles, Belgium
P. Barria, C. Caillol, B. Clerbaux, G. De Lentdecker, H. Delannoy, D. Dobur, G. Fasanella, L. Favart, A.P.R. Gay, A. Grebenyuk, T. Lenzi, A. Léonard, T. Maerschalk, A. Marinov, L. Perniè, A. Randle-conde, T. Reis, T. Seva, C. Vander Velde, P. Vanlaer, R. Yonamine, F. Zenoni, F. Zhang[3]

Ghent University, Ghent, Belgium
K. Beernaert, L. Benucci, A. Cimmino, S. Crucy, A. Fagot, G. Garcia, M. Gul, J. Mccartin, A.A. Ocampo Rios, D. Poyraz, D. Ryckbosch, S. Salva, M. Sigamani, N. Strobbe, M. Tytgat, W. Van Driessche, E. Yazgan, N. Zaganidis

Université Catholique de Louvain, Louvain-la-Neuve, Belgium
S. Basegmez, C. Beluffi[4], O. Bondu, S. Brochet, G. Bruno, R. Castello, A. Caudron, L. Ceard, G.G. Da Silveira, C. Delaere, D. Favart, L. Forthomme, A. Giammanco[5], J. Hollar, A. Jafari, P. Jez, M. Komm, V. Lemaitre, A. Mertens, C. Nuttens, L. Perrini, A. Pin, K. Piotrzkowski, A. Popov[6], L. Quertenmont, M. Selvaggi, M. Vidal Marono

Université de Mons, Mons, Belgium
N. Beliy, G.H. Hammad

Centro Brasileiro de Pesquisas Fisicas, Rio de Janeiro, Brazil
W.L. Aldá Júnior, G.A. Alves, L. Brito, M. Correa Martins Junior, T. Dos Reis Martins, C. Hensel, C. Mora Herrera, A. Moraes, M.E. Pol, P. Rebello Teles

Universidade do Estado do Rio de Janeiro, Rio de Janeiro, Brazil
E. Belchior Batista Das Chagas, W. Carvalho, J. Chinellato[7], A. Custódio, E.M. Da Costa, D. De Jesus Damiao, C. De Oliveira Martins, S. Fonseca De Souza, L.M. Huertas Guativa, H. Malbouisson, D. Matos Figueiredo, L. Mundim, H. Nogima, W.L. Prado Da Silva, A. Santoro, A. Sznajder, E.J. Tonelli Manganote[7], A. Vilela Pereira

Universidade Estadual Paulista [a], Universidade Federal do ABC [b], São Paulo, Brazil
S. Ahuja[a], C.A. Bernardes[b], A. De Souza Santos[b], S. Dogra[a], T.R. Fernandez Perez Tomei[a], E.M. Gregores[b], P.G. Mercadante[b], C.S. Moon[a,8], S.F. Novaes[a], Sandra S. Padula[a], D. Romero Abad, J.C. Ruiz Vargas

Institute for Nuclear Research and Nuclear Energy, Sofia, Bulgaria
A. Aleksandrov, V. Genchev[†], R. Hadjiiska, P. Iaydjiev, S. Piperov, M. Rodozov, S. Stoykova, G. Sultanov, M. Vutova

University of Sofia, Sofia, Bulgaria
A. Dimitrov, I. Glushkov, L. Litov, B. Pavlov, P. Petkov

Institute of High Energy Physics, Beijing, China
M. Ahmad, J.G. Bian, G.M. Chen, H.S. Chen, M. Chen, T. Cheng, R. Du, C.H. Jiang, R. Plestina[9], F. Romeo, S.M. Shaheen, J. Tao, C. Wang, Z. Wang, H. Zhang

State Key Laboratory of Nuclear Physics and Technology, Peking University, Beijing, China
C. Asawatangtrakuldee, Y. Ban, Q. Li, S. Liu, Y. Mao, S.J. Qian, D. Wang, Z. Xu, W. Zou

Universidad de Los Andes, Bogota, Colombia
C. Avila, A. Cabrera, L.F. Chaparro Sierra, C. Florez, J.P. Gomez, B. Gomez Moreno, J.C. Sanabria

University of Split, Faculty of Electrical Engineering, Mechanical Engineering and Naval Architecture, Split, Croatia
N. Godinovic, D. Lelas, D. Polic, I. Puljak

University of Split, Faculty of Science, Split, Croatia
Z. Antunovic, M. Kovac

Institute Rudjer Boskovic, Zagreb, Croatia
V. Brigljevic, K. Kadija, J. Luetic, L. Sudic

University of Cyprus, Nicosia, Cyprus
A. Attikis, G. Mavromanolakis, J. Mousa, C. Nicolaou, F. Ptochos, P.A. Razis, H. Rykaczewski

Charles University, Prague, Czech Republic
M. Bodlak, M. Finger[10], M. Finger Jr.[10]

Academy of Scientific Research and Technology of the Arab Republic of Egypt, Egyptian Network of High Energy Physics, Cairo, Egypt
R. Aly[11], E. El-khateeb[12], T. Elkafrawy[12], A. Lotfy[13], A. Mohamed[14], A. Radi[15,12], E. Salama[12,15], A. Sayed[12,15]

National Institute of Chemical Physics and Biophysics, Tallinn, Estonia
B. Calpas, M. Kadastik, M. Murumaa, M. Raidal, A. Tiko, C. Veelken

Department of Physics, University of Helsinki, Helsinki, Finland
P. Eerola, J. Pekkanen, M. Voutilainen

Helsinki Institute of Physics, Helsinki, Finland
J. Härkönen, V. Karimäki, R. Kinnunen, T. Lampén, K. Lassila-Perini, S. Lehti, T. Lindén, P. Luukka, T. Mäenpää, T. Peltola, E. Tuominen, J. Tuominiemi, E. Tuovinen, L. Wendland

Lappeenranta University of Technology, Lappeenranta, Finland
J. Talvitie, T. Tuuva

DSM/IRFU, CEA/Saclay, Gif-sur-Yvette, France
M. Besancon, F. Couderc, M. Dejardin, D. Denegri, B. Fabbro, J.L. Faure, C. Favaro, F. Ferri, S. Ganjour, A. Givernaud, P. Gras, G. Hamel de Monchenault, P. Jarry, E. Locci, M. Machet, J. Malcles, J. Rander, A. Rosowsky, M. Titov, A. Zghiche

Laboratoire Leprince-Ringuet, Ecole Polytechnique, IN2P3-CNRS, Palaiseau, France
S. Baffioni, F. Beaudette, P. Busson, L. Cadamuro, E. Chapon, C. Charlot, T. Dahms, O. Davignon, N. Filipovic, A. Florent, R. Granier de Cassagnac, S. Lisniak, L. Mastrolorenzo, P. Miné, I.N. Naranjo, M. Nguyen, C. Ochando, G. Ortona, P. Paganini, S. Regnard, R. Salerno, J.B. Sauvan, Y. Sirois, T. Strebler, Y. Yilmaz, A. Zabi

Institut Pluridisciplinaire Hubert Curien, Université de Strasbourg, Université de Haute Alsace Mulhouse, CNRS/IN2P3, Strasbourg, France
J.-L. Agram[16], J. Andrea, A. Aubin, D. Bloch, J.-M. Brom, M. Buttignol, E.C. Chabert, N. Chanon, C. Collard, E. Conte[16], X. Coubez, J.-C. Fontaine[16], D. Gelé, U. Goerlach, C. Goetzmann, A.-C. Le Bihan, J.A. Merlin[2], K. Skovpen, P. Van Hove

Centre de Calcul de l'Institut National de Physique Nucleaire et de Physique des Particules, CNRS/IN2P3, Villeurbanne, France
S. Gadrat

Université de Lyon, Université Claude Bernard Lyon 1, CNRS-IN2P3, Institut de Physique Nucléaire de Lyon, Villeurbanne, France
S. Beauceron, C. Bernet, G. Boudoul, E. Bouvier, C.A. Carrillo Montoya, J. Chasserat, R. Chierici, D. Contardo, B. Courbon, P. Depasse, H. El Mamouni, J. Fan, J. Fay, S. Gascon, M. Gouzevitch, B. Ille, I.B. Laktineh, M. Lethuillier, L. Mirabito, A.L. Pequegnot, S. Perries, J.D. Ruiz Alvarez, D. Sabes, L. Sgandurra, V. Sordini, M. Vander Donckt, P. Verdier, S. Viret, H. Xiao

Georgian Technical University, Tbilisi, Georgia
T. Toriashvili[17]

Institute of High Energy Physics and Informatization, Tbilisi State University, Tbilisi, Georgia
Z. Tsamalaidze[10]

RWTH Aachen University, I. Physikalisches Institut, Aachen, Germany
C. Autermann, S. Beranek, M. Edelhoff, L. Feld, A. Heister, M.K. Kiesel, K. Klein, M. Lipinski, A. Ostapchuk, M. Preuten, F. Raupach, J. Sammet, S. Schael, J.F. Schulte, T. Verlage, H. Weber, B. Wittmer, V. Zhukov[6]

RWTH Aachen University, III. Physikalisches Institut A, Aachen, Germany
M. Ata, M. Brodski, E. Dietz-Laursonn, D. Duchardt, M. Endres, M. Erdmann, S. Erdweg, T. Esch, R. Fischer, A. Güth, T. Hebbeker, C. Heidemann, K. Hoepfner, D. Klingebiel, S. Knutzen, P. Kreuzer, M. Merschmeyer, A. Meyer, P. Millet, M. Olschewski, K. Padeken, P. Papacz, T. Pook, M. Radziej, H. Reithler, M. Rieger, F. Scheuch, L. Sonnenschein, D. Teyssier, S. Thüer

RWTH Aachen University, III. Physikalisches Institut B, Aachen, Germany
V. Cherepanov, Y. Erdogan, G. Flügge, H. Geenen, M. Geisler, F. Hoehle, B. Kargoll, T. Kress, Y. Kuessel, A. Künsken, J. Lingemann[2], A. Nehrkorn, A. Nowack, I.M. Nugent, C. Pistone, O. Pooth, A. Stahl

Deutsches Elektronen-Synchrotron, Hamburg, Germany
M. Aldaya Martin, I. Asin, N. Bartosik, O. Behnke, U. Behrens, A.J. Bell, K. Borras,

A. Burgmeier, A. Cakir, L. Calligaris, A. Campbell, S. Choudhury, F. Costanza, C. Diez Pardos, G. Dolinska, S. Dooling, T. Dorland, G. Eckerlin, D. Eckstein, T. Eichhorn, G. Flucke, E. Gallo, J. Garay Garcia, A. Geiser, A. Gizhko, P. Gunnellini, J. Hauk, M. Hempel[18], H. Jung, A. Kalogeropoulos, O. Karacheban[18], M. Kasemann, P. Katsas, J. Kieseler, C. Kleinwort, I. Korol, W. Lange, J. Leonard, K. Lipka, A. Lobanov, W. Lohmann[18], R. Mankel, I. Marfin[18], I.-A. Melzer-Pellmann, A.B. Meyer, G. Mittag, J. Mnich, A. Mussgiller, S. Naumann-Emme, A. Nayak, E. Ntomari, H. Perrey, D. Pitzl, R. Placakyte, A. Raspereza, P.M. Ribeiro Cipriano, B. Roland, M.Ö. Sahin, P. Saxena, T. Schoerner-Sadenius, M. Schröder, C. Seitz, S. Spannagel, K.D. Trippkewitz, C. Wissing

University of Hamburg, Hamburg, Germany
V. Blobel, M. Centis Vignali, A.R. Draeger, J. Erfle, E. Garutti, K. Goebel, D. Gonzalez, M. Görner, J. Haller, M. Hoffmann, R.S. Höing, A. Junkes, R. Klanner, R. Kogler, T. Lapsien, T. Lenz, I. Marchesini, D. Marconi, D. Nowatschin, J. Ott, F. Pantaleo[2], T. Peiffer, A. Perieanu, N. Pietsch, J. Poehlsen, D. Rathjens, C. Sander, H. Schettler, P. Schleper, E. Schlieckau, A. Schmidt, J. Schwandt, M. Seidel, V. Sola, H. Stadie, G. Steinbrück, H. Tholen, D. Troendle, E. Usai, L. Vanelderen, A. Vanhoefer

Institut für Experimentelle Kernphysik, Karlsruhe, Germany
M. Akbiyik, C. Barth, C. Baus, J. Berger, C. Böser, E. Butz, T. Chwalek, F. Colombo, W. De Boer, A. Descroix, A. Dierlamm, M. Feindt, F. Frensch, M. Giffels, A. Gilbert, F. Hartmann[2], U. Husemann, F. Kassel[2], I. Katkov[6], A. Kornmayer[2], P. Lobelle Pardo, M.U. Mozer, T. Müller, Th. Müller, M. Plagge, G. Quast, K. Rabbertz, S. Röcker, F. Roscher, H.J. Simonis, F.M. Stober, R. Ulrich, J. Wagner-Kuhr, S. Wayand, T. Weiler, C. Wöhrmann, R. Wolf

Institute of Nuclear and Particle Physics (INPP), NCSR Demokritos, Aghia Paraskevi, Greece
G. Anagnostou, G. Daskalakis, T. Geralis, V.A. Giakoumopoulou, A. Kyriakis, D. Loukas, A. Markou, A. Psallidas, I. Topsis-Giotis

University of Athens, Athens, Greece
A. Agapitos, S. Kesisoglou, A. Panagiotou, N. Saoulidou, E. Tziaferi

University of Ioánnina, Ioánnina, Greece
I. Evangelou, G. Flouris, C. Foudas, P. Kokkas, N. Loukas, N. Manthos, I. Papadopoulos, E. Paradas, J. Strologas

Wigner Research Centre for Physics, Budapest, Hungary
G. Bencze, C. Hajdu, A. Hazi, P. Hidas, D. Horvath[19], F. Sikler, V. Veszpremi, G. Vesztergombi[20], A.J. Zsigmond

Institute of Nuclear Research ATOMKI, Debrecen, Hungary
N. Beni, S. Czellar, J. Karancsi[21], J. Molnar, Z. Szillasi

University of Debrecen, Debrecen, Hungary
M. Bartók[22], A. Makovec, P. Raics, Z.L. Trocsanyi, B. Ujvari

National Institute of Science Education and Research, Bhubaneswar, India
P. Mal, K. Mandal, N. Sahoo, S.K. Swain

Panjab University, Chandigarh, India
S. Bansal, S.B. Beri, V. Bhatnagar, R. Chawla, R. Gupta, U.Bhawandeep, A.K. Kalsi, A. Kaur, M. Kaur, R. Kumar, A. Mehta, M. Mittal, N. Nishu, J.B. Singh, G. Walia

University of Delhi, Delhi, India
Ashok Kumar, Arun Kumar, A. Bhardwaj, B.C. Choudhary, R.B. Garg, A. Kumar, S. Malhotra, M. Naimuddin, K. Ranjan, R. Sharma, V. Sharma

Saha Institute of Nuclear Physics, Kolkata, India
S. Banerjee, S. Bhattacharya, K. Chatterjee, S. Dey, S. Dutta, Sa. Jain, Sh. Jain, R. Khurana, N. Majumdar, A. Modak, K. Mondal, S. Mukherjee, S. Mukhopadhyay, A. Roy, D. Roy, S. Roy Chowdhury, S. Sarkar, M. Sharan

Bhabha Atomic Research Centre, Mumbai, India
A. Abdulsalam, R. Chudasama, D. Dutta, V. Jha, V. Kumar, A.K. Mohanty[2], L.M. Pant, P. Shukla, A. Topkar

Tata Institute of Fundamental Research, Mumbai, India
T. Aziz, S. Banerjee, S. Bhowmik[23], R.M. Chatterjee, R.K. Dewanjee, S. Dugad, S. Ganguly, S. Ghosh, M. Guchait, A. Gurtu[24], G. Kole, S. Kumar, B. Mahakud, M. Maity[23], G. Majumder, K. Mazumdar, S. Mitra, G.B. Mohanty, B. Parida, T. Sarkar[23], K. Sudhakar, N. Sur, B. Sutar, N. Wickramage[25]

Indian Institute of Science Education and Research (IISER), Pune, India
S. Sharma

Institute for Research in Fundamental Sciences (IPM), Tehran, Iran
H. Bakhshiansohi, H. Behnamian, S.M. Etesami[26], A. Fahim[27], R. Goldouzian, M. Khakzad, M. Mohammadi Najafabadi, M. Naseri, S. Paktinat Mehdiabadi, F. Rezaei Hosseinabadi, B. Safarzadeh[28], M. Zeinali

University College Dublin, Dublin, Ireland
M. Felcini, M. Grunewald

INFN Sezione di Bari [a], Università di Bari [b], Politecnico di Bari [c], Bari, Italy
M. Abbrescia[a,b], C. Calabria[a,b], C. Caputo[a,b], S.S. Chhibra[a,b], A. Colaleo[a], D. Creanza[a,c], L. Cristella[a,b], N. De Filippis[a,c], M. De Palma[a,b], L. Fiore[a], G. Iaselli[a,c], G. Maggi[a,c], M. Maggi[a], G. Miniello[a,b], S. My[a,c], S. Nuzzo[a,b], A. Pompili[a,b], G. Pugliese[a,c], R. Radogna[a,b], A. Ranieri[a], G. Selvaggi[a,b], L. Silvestris[a,2], R. Venditti[a,b], P. Verwilligen[a]

INFN Sezione di Bologna [a], Università di Bologna [b], Bologna, Italy
G. Abbiendi[a], C. Battilana[2], A.C. Benvenuti[a], D. Bonacorsi[a,b], S. Braibant-Giacomelli[a,b], L. Brigliadori[a,b], R. Campanini[a,b], P. Capiluppi[a,b], A. Castro[a,b], F.R. Cavallo[a], G. Codispoti[a,b], M. Cuffiani[a,b], G.M. Dallavalle[a], F. Fabbri[a], A. Fanfani[a,b], D. Fasanella[a,b], P. Giacomelli[a], C. Grandi[a], L. Guiducci[a,b], S. Marcellini[a], G. Masetti[a], A. Montanari[a], F.L. Navarria[a,b], A. Perrotta[a], A.M. Rossi[a,b], T. Rovelli[a,b], G.P. Siroli[a,b], N. Tosi[a,b], R. Travaglini[a,b]

INFN Sezione di Catania [a], Università di Catania [b], CSFNSM [c], Catania, Italy
G. Cappello[a], M. Chiorboli[a,b], S. Costa[a,b], F. Giordano[a], R. Potenza[a,b], A. Tricomi[a,b], C. Tuve[a,b]

INFN Sezione di Firenze [a], Università di Firenze [b], Firenze, Italy
G. Barbagli[a], V. Ciulli[a,b], C. Civinini[a], R. D'Alessandro[a,b], E. Focardi[a,b], S. Gonzi[a,b], V. Gori[a,b], P. Lenzi[a,b], M. Meschini[a], S. Paoletti[a], G. Sguazzoni[a], A. Tropiano[a,b], L. Viliani[a,b]

INFN Laboratori Nazionali di Frascati, Frascati, Italy
L. Benussi, S. Bianco, F. Fabbri, D. Piccolo

INFN Sezione di Genova [a], Università di Genova [b], Genova, Italy
V. Calvelli[a,b], F. Ferro[a], M. Lo Vetere[a,b], E. Robutti[a], S. Tosi[a,b]

INFN Sezione di Milano-Bicocca [a], Università di Milano-Bicocca [b], Milano, Italy
M.E. Dinardo[a,b], S. Fiorendi[a,b], S. Gennai[a], R. Gerosa[a,b], A. Ghezzi[a,b], P. Govoni[a,b], S. Malvezzi[a], R.A. Manzoni[a,b], B. Marzocchi[a,b,2], D. Menasce[a], L. Moroni[a], M. Paganoni[a,b], D. Pedrini[a], S. Ragazzi[a,b], N. Redaelli[a], T. Tabarelli de Fatis[a,b]

INFN Sezione di Napoli [a], Università di Napoli 'Federico II' [b], Napoli, Italy, Università della Basilicata [c], Potenza, Italy, Università G. Marconi [d], Roma, Italy
S. Buontempo[a], N. Cavallo[a,c], S. Di Guida[a,d,2], M. Esposito[a,b], F. Fabozzi[a,c], A.O.M. Iorio[a,b], G. Lanza[a], L. Lista[a], S. Meola[a,d,2], M. Merola[a], P. Paolucci[a,2], C. Sciacca[a,b], F. Thyssen

INFN Sezione di Padova [a], Università di Padova [b], Padova, Italy, Università di Trento [c], Trento, Italy
P. Azzi[a,2], N. Bacchetta[a], M. Bellato[a], D. Bisello[a,b], A. Branca[a,b], R. Carlin[a,b], P. Checchia[a], M. Dall'Osso[a,b,2], T. Dorigo[a], U. Dosselli[a], F. Gasparini[a,b], U. Gasparini[a,b], A. Gozzelino[a], M. Gulmini[a,29], K. Kanishchev[a,c], S. Lacaprara[a], M. Margoni[a,b], A.T. Meneguzzo[a,b], J. Pazzini[a,b], N. Pozzobon[a,b], P. Ronchese[a,b], F. Simonetto[a,b], E. Torassa[a], M. Tosi[a,b], S. Ventura[a], M. Zanetti, P. Zotto[a,b], A. Zucchetta[a,b,2]

INFN Sezione di Pavia [a], Università di Pavia [b], Pavia, Italy
A. Braghieri[a], A. Magnani[a], S.P. Ratti[a,b], V. Re[a], C. Riccardi[a,b], P. Salvini[a], I. Vai[a], P. Vitulo[a,b]

INFN Sezione di Perugia [a], Università di Perugia [b], Perugia, Italy
L. Alunni Solestizi[a,b], M. Biasini[a,b], G.M. Bilei[a], D. Ciangottini[a,b,2], L. Fanò[a,b], P. Lariccia[a,b], G. Mantovani[a,b], M. Menichelli[a], A. Saha[a], A. Santocchia[a,b], A. Spiezia[a,b]

INFN Sezione di Pisa [a], Università di Pisa [b], Scuola Normale Superiore di Pisa [c], Pisa, Italy
K. Androsov[a,30], P. Azzurri[a], G. Bagliesi[a], J. Bernardini[a], T. Boccali[a], G. Broccolo[a,c], R. Castaldi[a], M.A. Ciocci[a,30], R. Dell'Orso[a], S. Donato[a,c,2], G. Fedi, L. Foà[a,c†], A. Giassi[a], M.T. Grippo[a,30], F. Ligabue[a,c], T. Lomtadze[a], L. Martini[a,b], A. Messineo[a,b], F. Palla[a], A. Rizzi[a,b], A. Savoy-Navarro[a,31], A.T. Serban[a], P. Spagnolo[a], P. Squillacioti[a,30], R. Tenchini[a], G. Tonelli[a,b], A. Venturi[a], P.G. Verdini[a]

INFN Sezione di Roma [a], Università di Roma [b], Roma, Italy
L. Barone[a,b], F. Cavallari[a], G. D'imperio[a,b,2], D. Del Re[a,b], M. Diemoz[a], S. Gelli[a,b], C. Jorda[a], E. Longo[a,b], F. Margaroli[a,b], P. Meridiani[a], F. Micheli[a,b], G. Organtini[a,b], R. Paramatti[a], F. Preiato[a,b], S. Rahatlou[a,b], C. Rovelli[a], F. Santanastasio[a,b], P. Traczyk[a,b,2]

INFN Sezione di Torino [a], Università di Torino [b], Torino, Italy, Università del Piemonte Orientale [c], Novara, Italy
N. Amapane[a,b], R. Arcidiacono[a,c,2], S. Argiro[a,b], M. Arneodo[a,c], R. Bellan[a,b], C. Biino[a], N. Cartiglia[a], M. Costa[a,b], R. Covarelli[a,b], A. Degano[a,b], N. Demaria[a], L. Finco[a,b,2], B. Kiani[a,b], C. Mariotti[a], S. Maselli[a], E. Migliore[a,b], V. Monaco[a,b], E. Monteil[a,b], M. Musich[a], M.M. Obertino[a,b], L. Pacher[a,b], N. Pastrone[a], M. Pelliccioni[a], G.L. Pinna Angioni[a,b], F. Ravera[a,b], A. Romero[a,b], M. Ruspa[a,c], R. Sacchi[a,b], A. Solano[a,b], A. Staiano[a], U. Tamponi[a]

INFN Sezione di Trieste [a], Università di Trieste [b], Trieste, Italy
S. Belforte[a], V. Candelise[a,b,2], M. Casarsa[a], F. Cossutti[a], G. Della Ricca[a,b], B. Gobbo[a], C. La Licata[a,b], M. Marone[a,b], A. Schizzi[a,b], T. Umer[a,b], A. Zanetti[a]

Kangwon National University, Chunchon, Korea
S. Chang, A. Kropivnitskaya, S.K. Nam

Kyungpook National University, Daegu, Korea
D.H. Kim, G.N. Kim, M.S. Kim, D.J. Kong, S. Lee, Y.D. Oh, A. Sakharov, D.C. Son

Chonbuk National University, Jeonju, Korea
J.A. Brochero Cifuentes, H. Kim, T.J. Kim, M.S. Ryu

Chonnam National University, Institute for Universe and Elementary Particles, Kwangju, Korea
S. Song

Korea University, Seoul, Korea
S. Choi, Y. Go, D. Gyun, B. Hong, M. Jo, H. Kim, Y. Kim, B. Lee, K. Lee, K.S. Lee, S. Lee, S.K. Park, Y. Roh

Seoul National University, Seoul, Korea
H.D. Yoo

University of Seoul, Seoul, Korea
M. Choi, H. Kim, J.H. Kim, J.S.H. Lee, I.C. Park, G. Ryu

Sungkyunkwan University, Suwon, Korea
Y. Choi, Y.K. Choi, J. Goh, D. Kim, E. Kwon, J. Lee, I. Yu

Vilnius University, Vilnius, Lithuania
A. Juodagalvis, J. Vaitkus

National Centre for Particle Physics, Universiti Malaya, Kuala Lumpur, Malaysia
I. Ahmed, Z.A. Ibrahim, J.R. Komaragiri, M.A.B. Md Ali[32], F. Mohamad Idris[33], W.A.T. Wan Abdullah

Centro de Investigacion y de Estudios Avanzados del IPN, Mexico City, Mexico
E. Casimiro Linares, H. Castilla-Valdez, E. De La Cruz-Burelo, I. Heredia-de La Cruz[34], A. Hernandez-Almada, R. Lopez-Fernandez, A. Sanchez-Hernandez

Universidad Iberoamericana, Mexico City, Mexico
S. Carrillo Moreno, F. Vazquez Valencia

Benemerita Universidad Autonoma de Puebla, Puebla, Mexico
S. Carpinteyro, I. Pedraza, H.A. Salazar Ibarguen

Universidad Autónoma de San Luis Potosí, San Luis Potosí, Mexico
A. Morelos Pineda

University of Auckland, Auckland, New Zealand
D. Krofcheck

University of Canterbury, Christchurch, New Zealand
P.H. Butler, S. Reucroft

National Centre for Physics, Quaid-I-Azam University, Islamabad, Pakistan
A. Ahmad, M. Ahmad, Q. Hassan, H.R. Hoorani, W.A. Khan, T. Khurshid, M. Shoaib

National Centre for Nuclear Research, Swierk, Poland
H. Bialkowska, M. Bluj, B. Boimska, T. Frueboes, M. Górski, M. Kazana, K. Nawrocki, K. Romanowska-Rybinska, M. Szleper, P. Zalewski

Institute of Experimental Physics, Faculty of Physics, University of Warsaw, Warsaw, Poland
G. Brona, K. Bunkowski, K. Doroba, A. Kalinowski, M. Konecki, J. Krolikowski, M. Misiura, M. Olszewski, M. Walczak

Laboratório de Instrumentação e Física Experimental de Partículas, Lisboa, Portugal
P. Bargassa, C. Beirão Da Cruz E Silva, A. Di Francesco, P. Faccioli, P.G. Ferreira Parracho, M. Gallinaro, L. Lloret Iglesias, F. Nguyen, J. Rodrigues Antunes, J. Seixas, O. Toldaiev, D. Vadruccio, J. Varela, P. Vischia

Joint Institute for Nuclear Research, Dubna, Russia
S. Afanasiev, P. Bunin, M. Gavrilenko, I. Golutvin, I. Gorbunov, A. Kamenev, V. Karjavin, V. Konoplyanikov, A. Lanev, A. Malakhov, V. Matveev[35], P. Moisenz, V. Palichik, V. Perelygin, S. Shmatov, S. Shulha, N. Skatchkov, V. Smirnov, A. Zarubin

Petersburg Nuclear Physics Institute, Gatchina (St. Petersburg), Russia
V. Golovtsov, Y. Ivanov, V. Kim[36], E. Kuznetsova, P. Levchenko, V. Murzin, V. Oreshkin, I. Smirnov, V. Sulimov, L. Uvarov, S. Vavilov, A. Vorobyev

Institute for Nuclear Research, Moscow, Russia
Yu. Andreev, A. Dermenev, S. Gninenko, N. Golubev, A. Karneyeu, M. Kirsanov, N. Krasnikov, A. Pashenkov, D. Tlisov, A. Toropin

Institute for Theoretical and Experimental Physics, Moscow, Russia
V. Epshteyn, V. Gavrilov, N. Lychkovskaya, V. Popov, I. Pozdnyakov, G. Safronov, A. Spiridonov, E. Vlasov, A. Zhokin

National Research Nuclear University 'Moscow Engineering Physics Institute' (MEPhI), Moscow, Russia
A. Bylinkin

P.N. Lebedev Physical Institute, Moscow, Russia
V. Andreev, M. Azarkin[37], I. Dremin[37], M. Kirakosyan, A. Leonidov[37], G. Mesyats, S.V. Rusakov, A. Vinogradov

Skobeltsyn Institute of Nuclear Physics, Lomonosov Moscow State University, Moscow, Russia
A. Baskakov, A. Belyaev, E. Boos, V. Bunichev, M. Dubinin[38], L. Dudko, A. Ershov, A. Gribushin, V. Klyukhin, O. Kodolova, I. Lokhtin, I. Myagkov, S. Obraztsov, S. Petrushanko, V. Savrin

State Research Center of Russian Federation, Institute for High Energy Physics, Protvino, Russia
I. Azhgirey, I. Bayshev, S. Bitioukov, V. Kachanov, A. Kalinin, D. Konstantinov, V. Krychkine, V. Petrov, R. Ryutin, A. Sobol, L. Tourtchanovitch, S. Troshin, N. Tyurin, A. Uzunian, A. Volkov

University of Belgrade, Faculty of Physics and Vinca Institute of Nuclear Sciences, Belgrade, Serbia
P. Adzic[39], M. Ekmedzic, J. Milosevic, V. Rekovic

Centro de Investigaciones Energéticas Medioambientales y Tecnológicas (CIEMAT), Madrid, Spain
J. Alcaraz Maestre, E. Calvo, M. Cerrada, M. Chamizo Llatas, N. Colino, B. De La Cruz, A. Delgado Peris, D. Domínguez Vázquez, A. Escalante Del Valle, C. Fernandez Bedoya, J.P. Fernández Ramos, J. Flix, M.C. Fouz, P. Garcia-Abia, O. Gonzalez Lopez, S. Goy Lopez, J.M. Hernandez, M.I. Josa, E. Navarro De Martino, A. Pérez-Calero Yzquierdo, J. Puerta Pelayo, A. Quintario Olmeda, I. Redondo, L. Romero, M.S. Soares

Universidad Autónoma de Madrid, Madrid, Spain
C. Albajar, J.F. de Trocóniz, M. Missiroli, D. Moran

Universidad de Oviedo, Oviedo, Spain
H. Brun, J. Cuevas, J. Fernandez Menendez, S. Folgueras, I. Gonzalez Caballero, E. Palencia Cortezon, J.M. Vizan Garcia

Instituto de Física de Cantabria (IFCA), CSIC-Universidad de Cantabria, Santander, Spain
I.J. Cabrillo, A. Calderon, J.R. Castiñeiras De Saa, P. De Castro Manzano, J. Duarte Campderros, M. Fernandez, G. Gomez, A. Graziano, A. Lopez Virto, J. Marco, R. Marco, C. Martinez Rivero, F. Matorras, F.J. Munoz Sanchez, J. Piedra Gomez, T. Rodrigo, A.Y. Rodríguez-Marrero, A. Ruiz-Jimeno, L. Scodellaro, I. Vila, R. Vilar Cortabitarte

CERN, European Organization for Nuclear Research, Geneva, Switzerland
D. Abbaneo, E. Auffray, G. Auzinger, M. Bachtis, P. Baillon, A.H. Ball, D. Barney, A. Benaglia, J. Bendavid, L. Benhabib, J.F. Benitez, G.M. Berruti, G. Bianchi, P. Bloch, A. Bocci, A. Bonato, C. Botta, H. Breuker, T. Camporesi, G. Cerminara, S. Colafranceschi[40], M. D'Alfonso, D. d'Enterria, A. Dabrowski, V. Daponte, A. David, M. De Gruttola, F. De Guio, A. De Roeck, S. De Visscher, E. Di Marco, M. Dobson, M. Dordevic, T. du Pree, N. Dupont, A. Elliott-Peisert, J. Eugster, G. Franzoni, W. Funk, D. Gigi, K. Gill, D. Giordano, M. Girone, F. Glege, R. Guida, S. Gundacker, M. Guthoff, J. Hammer, M. Hansen, P. Harris, J. Hegeman, V. Innocente, P. Janot, H. Kirschenmann, M.J. Kortelainen, K. Kousouris, K. Krajczar, P. Lecoq, C. Lourenço, M.T. Lucchini, N. Magini, L. Malgeri, M. Mannelli, J. Marrouche, A. Martelli, L. Masetti, F. Meijers, S. Mersi, E. Meschi, F. Moortgat, S. Morovic, M. Mulders, M.V. Nemallapudi, H. Neugebauer, S. Orfanelli[41], L. Orsini, L. Pape, E. Perez, A. Petrilli, G. Petrucciani, A. Pfeiffer, D. Piparo, A. Racz, G. Rolandi[42], M. Rovere, M. Ruan, H. Sakulin, C. Schäfer, C. Schwick, A. Sharma, P. Silva, M. Simon, P. Sphicas[43], D. Spiga, J. Steggemann, B. Stieger, M. Stoye, Y. Takahashi, D. Treille, A. Tsirou, G.I. Veres[20], N. Wardle, H.K. Wöhri, A. Zagozdzinska[44], W.D. Zeuner

Paul Scherrer Institut, Villigen, Switzerland
W. Bertl, K. Deiters, W. Erdmann, R. Horisberger, Q. Ingram, H.C. Kaestli, D. Kotlinski, U. Langenegger, D. Renker, T. Rohe

Institute for Particle Physics, ETH Zurich, Zurich, Switzerland
F. Bachmair, L. Bäni, L. Bianchini, M.A. Buchmann, B. Casal, G. Dissertori, M. Dittmar, M. Donegà, M. Dünser, P. Eller, C. Grab, C. Heidegger, D. Hits, J. Hoss, G. Kasieczka, W. Lustermann, B. Mangano, A.C. Marini, M. Marionneau, P. Martinez Ruiz del Arbol, M. Masciovecchio, D. Meister, P. Musella, F. Nessi-Tedaldi, F. Pandolfi, J. Pata, F. Pauss, L. Perrozzi, M. Peruzzi, M. Quittnat, M. Rossini, A. Starodumov[45], M. Takahashi, V.R. Tavolaro, K. Theofilatos, R. Wallny, H.A. Weber

Universität Zürich, Zurich, Switzerland
T.K. Aarrestad, C. Amsler[46], L. Caminada, M.F. Canelli, V. Chiochia, A. De Cosa, C. Galloni, A. Hinzmann, T. Hreus, B. Kilminster, C. Lange, J. Ngadiuba, D. Pinna, P. Robmann, F.J. Ronga, D. Salerno, S. Taroni, Y. Yang

National Central University, Chung-Li, Taiwan
M. Cardaci, K.H. Chen, T.H. Doan, C. Ferro, M. Konyushikhin, C.M. Kuo, W. Lin, Y.J. Lu, R. Volpe, S.S. Yu

National Taiwan University (NTU), Taipei, Taiwan
R. Bartek, P. Chang, Y.H. Chang, Y.W. Chang, Y. Chao, K.F. Chen, P.H. Chen, C. Dietz, F. Fiori, U. Grundler, W.-S. Hou, Y. Hsiung, Y.F. Liu, R.-S. Lu, M. Miñano Moya, E. Petrakou, J.F. Tsai, Y.M. Tzeng

Chulalongkorn University, Faculty of Science, Department of Physics, Bangkok, Thailand
B. Asavapibhop, K. Kovitanggoon, G. Singh, N. Srimanobhas, N. Suwonjandee

Cukurova University, Adana, Turkey
A. Adiguzel, M.N. Bakirci[47], C. Dozen, I. Dumanoglu, E. Eskut, S. Girgis, G. Gokbulut, Y. Guler, E. Gurpinar, I. Hos, E.E. Kangal[48], G. Onengut[49], K. Ozdemir[50], A. Polatoz, D. Sunar Cerci[51], M. Vergili, C. Zorbilmez

Middle East Technical University, Physics Department, Ankara, Turkey
I.V. Akin, B. Bilin, S. Bilmis, B. Isildak[52], G. Karapinar[53], U.E. Surat, M. Yalvac, M. Zeyrek

Bogazici University, Istanbul, Turkey
E.A. Albayrak[54], E. Gülmez, M. Kaya[55], O. Kaya[56], T. Yetkin[57]

Istanbul Technical University, Istanbul, Turkey
K. Cankocak, S. Sen[58], F.I. Vardarlı

Institute for Scintillation Materials of National Academy of Science of Ukraine, Kharkov, Ukraine
B. Grynyov

National Scientific Center, Kharkov Institute of Physics and Technology, Kharkov, Ukraine
L. Levchuk, P. Sorokin

University of Bristol, Bristol, United Kingdom
R. Aggleton, F. Ball, L. Beck, J.J. Brooke, E. Clement, D. Cussans, H. Flacher, J. Goldstein, M. Grimes, G.P. Heath, H.F. Heath, J. Jacob, L. Kreczko, C. Lucas, Z. Meng, D.M. Newbold[59], S. Paramesvaran, A. Poll, T. Sakuma, S. Seif El Nasr-storey, S. Senkin, D. Smith, V.J. Smith

Rutherford Appleton Laboratory, Didcot, United Kingdom
K.W. Bell, A. Belyaev[60], C. Brew, R.M. Brown, D.J.A. Cockerill, J.A. Coughlan, K. Harder, S. Harper, E. Olaiya, D. Petyt, C.H. Shepherd-Themistocleous, A. Thea, L. Thomas, I.R. Tomalin, T. Williams, W.J. Womersley, S.D. Worm

Imperial College, London, United Kingdom
M. Baber, R. Bainbridge, O. Buchmuller, A. Bundock, D. Burton, S. Casasso, M. Citron, D. Colling, L. Corpe, N. Cripps, P. Dauncey, G. Davies, A. De Wit, M. Della Negra, P. Dunne, A. Elwood, W. Ferguson, J. Fulcher, D. Futyan, G. Hall, G. Iles, G. Karapostoli, M. Kenzie, R. Lane, R. Lucas[59], L. Lyons, A.-M. Magnan, S. Malik, J. Nash, A. Nikitenko[45], J. Pela, M. Pesaresi, K. Petridis, D.M. Raymond, A. Richards, A. Rose, C. Seez, A. Tapper, K. Uchida, M. Vazquez Acosta[61], T. Virdee, S.C. Zenz

Brunel University, Uxbridge, United Kingdom
J.E. Cole, P.R. Hobson, A. Khan, P. Kyberd, D. Leggat, D. Leslie, I.D. Reid, P. Symonds, L. Teodorescu, M. Turner

Baylor University, Waco, USA
A. Borzou, J. Dittmann, K. Hatakeyama, A. Kasmi, H. Liu, N. Pastika

The University of Alabama, Tuscaloosa, USA
O. Charaf, S.I. Cooper, C. Henderson, P. Rumerio

Boston University, Boston, USA
A. Avetisyan, T. Bose, C. Fantasia, D. Gastler, P. Lawson, D. Rankin, C. Richardson, J. Rohlf, J. St. John, L. Sulak, D. Zou

Brown University, Providence, USA
J. Alimena, E. Berry, S. Bhattacharya, D. Cutts, N. Dhingra, A. Ferapontov, A. Garabedian, U. Heintz, E. Laird, G. Landsberg, Z. Mao, M. Narain, S. Sagir, T. Sinthuprasith

University of California, Davis, Davis, USA
R. Breedon, G. Breto, M. Calderon De La Barca Sanchez, S. Chauhan, M. Chertok, J. Conway, R. Conway, P.T. Cox, R. Erbacher, M. Gardner, W. Ko, R. Lander, M. Mulhearn, D. Pellett, J. Pilot, F. Ricci-Tam, S. Shalhout, J. Smith, M. Squires, D. Stolp, M. Tripathi, S. Wilbur, R. Yohay

University of California, Los Angeles, USA
R. Cousins, P. Everaerts, C. Farrell, J. Hauser, M. Ignatenko, G. Rakness, D. Saltzberg, E. Takasugi, V. Valuev, M. Weber

University of California, Riverside, Riverside, USA
K. Burt, R. Clare, J. Ellison, J.W. Gary, G. Hanson, J. Heilman, M. Ivova PANEVA, P. Jandir, E. Kennedy, F. Lacroix, O.R. Long, A. Luthra, M. Malberti, M. Olmedo Negrete, A. Shrinivas, H. Wei, S. Wimpenny

University of California, San Diego, La Jolla, USA
J.G. Branson, G.B. Cerati, S. Cittolin, R.T. D'Agnolo, A. Holzner, R. Kelley, D. Klein, J. Letts, I. Macneill, D. Olivito, S. Padhi, M. Pieri, M. Sani, V. Sharma, S. Simon, M. Tadel, Y. Tu, A. Vartak, S. Wasserbaech[62], C. Welke, F. Würthwein, A. Yagil, G. Zevi Della Porta

University of California, Santa Barbara, Santa Barbara, USA
D. Barge, J. Bradmiller-Feld, C. Campagnari, A. Dishaw, V. Dutta, K. Flowers, M. Franco Sevilla, P. Geffert, C. George, F. Golf, L. Gouskos, J. Gran, J. Incandela, C. Justus, N. Mccoll, S.D. Mullin, J. Richman, D. Stuart, I. Suarez, W. To, C. West, J. Yoo

California Institute of Technology, Pasadena, USA
D. Anderson, A. Apresyan, A. Bornheim, J. Bunn, Y. Chen, J. Duarte, A. Mott, H.B. Newman, C. Pena, M. Pierini, M. Spiropulu, J.R. Vlimant, S. Xie, R.Y. Zhu

Carnegie Mellon University, Pittsburgh, USA
V. Azzolini, A. Calamba, B. Carlson, T. Ferguson, Y. Iiyama, M. Paulini, J. Russ, M. Sun, H. Vogel, I. Vorobiev

University of Colorado Boulder, Boulder, USA
J.P. Cumalat, W.T. Ford, A. Gaz, F. Jensen, A. Johnson, M. Krohn, T. Mulholland, U. Nauenberg, J.G. Smith, K. Stenson, S.R. Wagner

Cornell University, Ithaca, USA
J. Alexander, A. Chatterjee, J. Chaves, J. Chu, S. Dittmer, N. Eggert, N. Mirman, G. Nicolas Kaufman, J.R. Patterson, A. Rinkevicius, A. Ryd, L. Skinnari, L. Soffi, W. Sun, S.M. Tan, W.D. Teo, J. Thom, J. Thompson, J. Tucker, Y. Weng, P. Wittich

Fermi National Accelerator Laboratory, Batavia, USA
S. Abdullin, M. Albrow, J. Anderson, G. Apollinari, L.A.T. Bauerdick, A. Beretvas, J. Berryhill, P.C. Bhat, G. Bolla, K. Burkett, J.N. Butler, H.W.K. Cheung, F. Chlebana, S. Cihangir, V.D. Elvira, I. Fisk, J. Freeman, E. Gottschalk, L. Gray, D. Green, S. Grünendahl, O. Gutsche, J. Hanlon, D. Hare, R.M. Harris, J. Hirschauer, B. Hooberman, Z. Hu, S. Jindariani, M. Johnson, U. Joshi, A.W. Jung, B. Klima, B. Kreis, S. Kwan[†], S. Lammel, J. Linacre, D. Lincoln, R. Lipton, T. Liu, R. Lopes De Sá, J. Lykken, K. Maeshima, J.M. Marraffino, V.I. Martinez Outschoorn, S. Maruyama, D. Mason, P. McBride, P. Merkel, K. Mishra, S. Mrenna, S. Nahn, C. Newman-Holmes, V. O'Dell, O. Prokofyev, E. Sexton-Kennedy, A. Soha, W.J. Spalding, L. Spiegel,

L. Taylor, S. Tkaczyk, N.V. Tran, L. Uplegger, E.W. Vaandering, C. Vernieri, M. Verzocchi, R. Vidal, A. Whitbeck, F. Yang, H. Yin

University of Florida, Gainesville, USA
D. Acosta, P. Avery, P. Bortignon, D. Bourilkov, A. Carnes, M. Carver, D. Curry, S. Das, G.P. Di Giovanni, R.D. Field, M. Fisher, I.K. Furic, J. Hugon, J. Konigsberg, A. Korytov, J.F. Low, P. Ma, K. Matchev, H. Mei, P. Milenovic[63], G. Mitselmakher, L. Muniz, D. Rank, R. Rossin, L. Shchutska, M. Snowball, D. Sperka, J. Wang, S. Wang, J. Yelton

Florida International University, Miami, USA
S. Hewamanage, S. Linn, P. Markowitz, G. Martinez, J.L. Rodriguez

Florida State University, Tallahassee, USA
A. Ackert, J.R. Adams, T. Adams, A. Askew, J. Bochenek, B. Diamond, J. Haas, S. Hagopian, V. Hagopian, K.F. Johnson, A. Khatiwada, H. Prosper, V. Veeraraghavan, M. Weinberg

Florida Institute of Technology, Melbourne, USA
V. Bhopatkar, M. Hohlmann, H. Kalakhety, D. Mareskas-palcek, T. Roy, F. Yumiceva

University of Illinois at Chicago (UIC), Chicago, USA
M.R. Adams, L. Apanasevich, D. Berry, R.R. Betts, I. Bucinskaite, R. Cavanaugh, O. Evdokimov, L. Gauthier, C.E. Gerber, D.J. Hofman, P. Kurt, C. O'Brien, I.D. Sandoval Gonzalez, C. Silkworth, P. Turner, N. Varelas, Z. Wu, M. Zakaria

The University of Iowa, Iowa City, USA
B. Bilki[64], W. Clarida, K. Dilsiz, S. Durgut, R.P. Gandrajula, M. Haytmyradov, V. Khristenko, J.-P. Merlo, H. Mermerkaya[65], A. Mestvirishvili, A. Moeller, J. Nachtman, H. Ogul, Y. Onel, F. Ozok[54], A. Penzo, C. Snyder, P. Tan, E. Tiras, J. Wetzel, K. Yi

Johns Hopkins University, Baltimore, USA
I. Anderson, B.A. Barnett, B. Blumenfeld, D. Fehling, L. Feng, A.V. Gritsan, P. Maksimovic, C. Martin, K. Nash, M. Osherson, M. Swartz, M. Xiao, Y. Xin

The University of Kansas, Lawrence, USA
P. Baringer, A. Bean, G. Benelli, C. Bruner, J. Gray, R.P. Kenny III, D. Majumder, M. Malek, M. Murray, D. Noonan, S. Sanders, R. Stringer, Q. Wang, J.S. Wood

Kansas State University, Manhattan, USA
I. Chakaberia, A. Ivanov, K. Kaadze, S. Khalil, M. Makouski, Y. Maravin, A. Mohammadi, L.K. Saini, N. Skhirtladze, I. Svintradze, S. Toda

Lawrence Livermore National Laboratory, Livermore, USA
D. Lange, F. Rebassoo, D. Wright

University of Maryland, College Park, USA
C. Anelli, A. Baden, O. Baron, A. Belloni, B. Calvert, S.C. Eno, C. Ferraioli, J.A. Gomez, N.J. Hadley, S. Jabeen, R.G. Kellogg, T. Kolberg, J. Kunkle, Y. Lu, A.C. Mignerey, K. Pedro, Y.H. Shin, A. Skuja, M.B. Tonjes, S.C. Tonwar

Massachusetts Institute of Technology, Cambridge, USA
A. Apyan, R. Barbieri, A. Baty, K. Bierwagen, S. Brandt, W. Busza, I.A. Cali, Z. Demiragli, L. Di Matteo, G. Gomez Ceballos, M. Goncharov, D. Gulhan, G.M. Innocenti, M. Klute, D. Kovalskyi, Y.S. Lai, Y.-J. Lee, A. Levin, P.D. Luckey, C. Mcginn, C. Mironov, X. Niu, C. Paus, D. Ralph, C. Roland, G. Roland, J. Salfeld-Nebgen, G.S.F. Stephans, K. Sumorok, M. Varma, D. Velicanu, J. Veverka, J. Wang, T.W. Wang, B. Wyslouch, M. Yang, V. Zhukova

University of Minnesota, Minneapolis, USA
B. Dahmes, A. Finkel, A. Gude, P. Hansen, S. Kalafut, S.C. Kao, K. Klapoetke, Y. Kubota, Z. Lesko, J. Mans, S. Nourbakhsh, N. Ruckstuhl, R. Rusack, N. Tambe, J. Turkewitz

University of Mississippi, Oxford, USA
J.G. Acosta, S. Oliveros

University of Nebraska-Lincoln, Lincoln, USA
E. Avdeeva, K. Bloom, S. Bose, D.R. Claes, A. Dominguez, C. Fangmeier, R. Gonzalez Suarez, R. Kamalieddin, J. Keller, D. Knowlton, I. Kravchenko, J. Lazo-Flores, F. Meier, J. Monroy, F. Ratnikov, J.E. Siado, G.R. Snow

State University of New York at Buffalo, Buffalo, USA
M. Alyari, J. Dolen, J. George, A. Godshalk, I. Iashvili, J. Kaisen, A. Kharchilava, A. Kumar, S. Rappoccio

Northeastern University, Boston, USA
G. Alverson, E. Barberis, D. Baumgartel, M. Chasco, A. Hortiangtham, A. Massironi, D.M. Morse, D. Nash, T. Orimoto, R. Teixeira De Lima, D. Trocino, R.-J. Wang, D. Wood, J. Zhang

Northwestern University, Evanston, USA
K.A. Hahn, A. Kubik, N. Mucia, N. Odell, B. Pollack, A. Pozdnyakov, M. Schmitt, S. Stoynev, K. Sung, M. Trovato, M. Velasco, S. Won

University of Notre Dame, Notre Dame, USA
A. Brinkerhoff, N. Dev, M. Hildreth, C. Jessop, D.J. Karmgard, N. Kellams, K. Lannon, S. Lynch, N. Marinelli, F. Meng, C. Mueller, Y. Musienko[35], T. Pearson, M. Planer, R. Ruchti, G. Smith, N. Valls, M. Wayne, M. Wolf, A. Woodard

The Ohio State University, Columbus, USA
L. Antonelli, J. Brinson, B. Bylsma, L.S. Durkin, S. Flowers, A. Hart, C. Hill, R. Hughes, K. Kotov, T.Y. Ling, B. Liu, W. Luo, D. Puigh, M. Rodenburg, B.L. Winer, H.W. Wulsin

Princeton University, Princeton, USA
O. Driga, P. Elmer, J. Hardenbrook, P. Hebda, S.A. Koay, P. Lujan, D. Marlow, T. Medvedeva, M. Mooney, J. Olsen, C. Palmer, P. Piroué, X. Quan, H. Saka, D. Stickland, C. Tully, J.S. Werner, A. Zuranski

Purdue University, West Lafayette, USA
V.E. Barnes, D. Benedetti, D. Bortoletto, L. Gutay, M.K. Jha, M. Jones, K. Jung, M. Kress, N. Leonardo, D.H. Miller, N. Neumeister, F. Primavera, B.C. Radburn-Smith, X. Shi, I. Shipsey, D. Silvers, J. Sun, A. Svyatkovskiy, F. Wang, W. Xie, L. Xu, J. Zablocki

Purdue University Calumet, Hammond, USA
N. Parashar, J. Stupak

Rice University, Houston, USA
A. Adair, B. Akgun, Z. Chen, K.M. Ecklund, F.J.M. Geurts, M. Guilbaud, W. Li, B. Michlin, M. Northup, B.P. Padley, R. Redjimi, J. Roberts, J. Rorie, Z. Tu, J. Zabel

University of Rochester, Rochester, USA
B. Betchart, A. Bodek, P. de Barbaro, R. Demina, Y. Eshaq, T. Ferbel, M. Galanti, A. Garcia-Bellido, P. Goldenzweig, J. Han, A. Harel, O. Hindrichs, A. Khukhunaishvili, G. Petrillo, M. Verzetti

The Rockefeller University, New York, USA
L. Demortier

Rutgers, The State University of New Jersey, Piscataway, USA
S. Arora, A. Barker, J.P. Chou, C. Contreras-Campana, E. Contreras-Campana, D. Duggan, D. Ferencek, Y. Gershtein, R. Gray, E. Halkiadakis, D. Hidas, E. Hughes, S. Kaplan, R. Kunnawalkam Elayavalli, A. Lath, S. Panwalkar, M. Park, S. Salur, S. Schnetzer, D. Sheffield, S. Somalwar, R. Stone, S. Thomas, P. Thomassen, M. Walker

University of Tennessee, Knoxville, USA
M. Foerster, G. Riley, K. Rose, S. Spanier, A. York

Texas A&M University, College Station, USA
O. Bouhali[66], A. Castaneda Hernandez, M. Dalchenko, M. De Mattia, A. Delgado, S. Dildick, R. Eusebi, W. Flanagan, J. Gilmore, T. Kamon[67], V. Krutelyov, R. Montalvo, R. Mueller, I. Osipenkov, Y. Pakhotin, R. Patel, A. Perloff, J. Roe, A. Rose, A. Safonov, A. Tatarinov, K.A. Ulmer[2]

Texas Tech University, Lubbock, USA
N. Akchurin, C. Cowden, J. Damgov, C. Dragoiu, P.R. Dudero, J. Faulkner, S. Kunori, K. Lamichhane, S.W. Lee, T. Libeiro, S. Undleeb, I. Volobouev

Vanderbilt University, Nashville, USA
E. Appelt, A.G. Delannoy, S. Greene, A. Gurrola, R. Janjam, W. Johns, C. Maguire, Y. Mao, A. Melo, P. Sheldon, B. Snook, S. Tuo, J. Velkovska, Q. Xu

University of Virginia, Charlottesville, USA
M.W. Arenton, S. Boutle, B. Cox, B. Francis, J. Goodell, R. Hirosky, A. Ledovskoy, H. Li, C. Lin, C. Neu, E. Wolfe, J. Wood, F. Xia

Wayne State University, Detroit, USA
C. Clarke, R. Harr, P.E. Karchin, C. Kottachchi Kankanamge Don, P. Lamichhane, J. Sturdy

University of Wisconsin, Madison, USA
D.A. Belknap, D. Carlsmith, M. Cepeda, A. Christian, S. Dasu, L. Dodd, S. Duric, E. Friis, B. Gomber, R. Hall-Wilton, M. Herndon, A. Hervé, P. Klabbers, A. Lanaro, A. Levine, K. Long, R. Loveless, A. Mohapatra, I. Ojalvo, T. Perry, G.A. Pierro, G. Polese, I. Ross, T. Ruggles, T. Sarangi, A. Savin, A. Sharma, N. Smith, W.H. Smith, D. Taylor, N. Woods

†: Deceased
1: Also at Vienna University of Technology, Vienna, Austria
2: Also at CERN, European Organization for Nuclear Research, Geneva, Switzerland
3: Also at State Key Laboratory of Nuclear Physics and Technology, Peking University, Beijing, China
4: Also at Institut Pluridisciplinaire Hubert Curien, Université de Strasbourg, Université de Haute Alsace Mulhouse, CNRS/IN2P3, Strasbourg, France
5: Also at National Institute of Chemical Physics and Biophysics, Tallinn, Estonia
6: Also at Skobeltsyn Institute of Nuclear Physics, Lomonosov Moscow State University, Moscow, Russia
7: Also at Universidade Estadual de Campinas, Campinas, Brazil
8: Also at Centre National de la Recherche Scientifique (CNRS) - IN2P3, Paris, France
9: Also at Laboratoire Leprince-Ringuet, Ecole Polytechnique, IN2P3-CNRS, Palaiseau, France
10: Also at Joint Institute for Nuclear Research, Dubna, Russia
11: Now at Helwan University, Cairo, Egypt

12: Now at Ain Shams University, Cairo, Egypt
13: Now at Fayoum University, El-Fayoum, Egypt
14: Also at Zewail City of Science and Technology, Zewail, Egypt
15: Also at British University in Egypt, Cairo, Egypt
16: Also at Université de Haute Alsace, Mulhouse, France
17: Also at Institute of High Energy Physics and Informatization, Tbilisi State University, Tbilisi, Georgia
18: Also at Brandenburg University of Technology, Cottbus, Germany
19: Also at Institute of Nuclear Research ATOMKI, Debrecen, Hungary
20: Also at Eötvös Loránd University, Budapest, Hungary
21: Also at University of Debrecen, Debrecen, Hungary
22: Also at Wigner Research Centre for Physics, Budapest, Hungary
23: Also at University of Visva-Bharati, Santiniketan, India
24: Now at King Abdulaziz University, Jeddah, Saudi Arabia
25: Also at University of Ruhuna, Matara, Sri Lanka
26: Also at Isfahan University of Technology, Isfahan, Iran
27: Also at University of Tehran, Department of Engineering Science, Tehran, Iran
28: Also at Plasma Physics Research Center, Science and Research Branch, Islamic Azad University, Tehran, Iran
29: Also at Laboratori Nazionali di Legnaro dell'INFN, Legnaro, Italy
30: Also at Università degli Studi di Siena, Siena, Italy
31: Also at Purdue University, West Lafayette, USA
32: Also at International Islamic University of Malaysia, Kuala Lumpur, Malaysia
33: Also at Malaysian Nuclear Agency, MOSTI, Kajang, Malaysia
34: Also at CONSEJO NATIONAL DE CIENCIA Y TECNOLOGIA, MEXICO, Mexico
35: Also at Institute for Nuclear Research, Moscow, Russia
36: Also at St. Petersburg State Polytechnical University, St. Petersburg, Russia
37: Also at National Research Nuclear University 'Moscow Engineering Physics Institute' (MEPhI), Moscow, Russia
38: Also at California Institute of Technology, Pasadena, USA
39: Also at Faculty of Physics, University of Belgrade, Belgrade, Serbia
40: Also at Facoltà Ingegneria, Università di Roma, Roma, Italy
41: Also at National Technical University of Athens, Athens, Greece
42: Also at Scuola Normale e Sezione dell'INFN, Pisa, Italy
43: Also at University of Athens, Athens, Greece
44: Also at Warsaw University of Technology, Institute of Electronic Systems, Warsaw, Poland
45: Also at Institute for Theoretical and Experimental Physics, Moscow, Russia
46: Also at Albert Einstein Center for Fundamental Physics, Bern, Switzerland
47: Also at Gaziosmanpasa University, Tokat, Turkey
48: Also at Mersin University, Mersin, Turkey
49: Also at Cag University, Mersin, Turkey
50: Also at Piri Reis University, Istanbul, Turkey
51: Also at Adiyaman University, Adiyaman, Turkey
52: Also at Ozyegin University, Istanbul, Turkey
53: Also at Izmir Institute of Technology, Izmir, Turkey
54: Also at Mimar Sinan University, Istanbul, Istanbul, Turkey
55: Also at Marmara University, Istanbul, Turkey
56: Also at Kafkas University, Kars, Turkey
57: Also at Yildiz Technical University, Istanbul, Turkey

58: Also at Hacettepe University, Ankara, Turkey
59: Also at Rutherford Appleton Laboratory, Didcot, United Kingdom
60: Also at School of Physics and Astronomy, University of Southampton, Southampton, United Kingdom
61: Also at Instituto de Astrofísica de Canarias, La Laguna, Spain
62: Also at Utah Valley University, Orem, USA
63: Also at University of Belgrade, Faculty of Physics and Vinca Institute of Nuclear Sciences, Belgrade, Serbia
64: Also at Argonne National Laboratory, Argonne, USA
65: Also at Erzincan University, Erzincan, Turkey
66: Also at Texas A&M University at Qatar, Doha, Qatar
67: Also at Kyungpook National University, Daegu, Korea